NeuroImage 328 (2026) 121774

Contents lists available at ScienceDirect

NeuroImage

journal homepage: www.elsevier.com/locate/ynimg

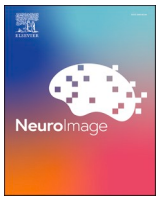

Decoding haptic and imagined stimulus size in the human cortex

Samantha Sartin [a], Federica Danaj [a,b], Fabio Del Giudice [a], Juan Chen [c], Dietrich Samuel Schwarzkopf [d,e], Irene Sperandio [f], Simona Monaco [a,*]

[a] Center for Mind/Brain Sciences (CIMeC), University of Trento, Trento, Italy
[b] University of Regensburg, Regensburg, Germany
[c] School of Psychology, South China Normal University, Guangzhou, Guangdong Province 510631, China
[d] School of Optometry & Vision Science, University of Auckland, New Zealand
[e] Experimental Psychology, University College London, United Kingdom
[f] Department of Psychology and Cognitive Science (DiPSCo), University of Trento, Trento, Italy

ARTICLE INFO

keywords:
Size
Haptic exploration
Visual imagery
Early visual cortex
Functional magnetic resonance imaging (fMRI)
Multivoxel pattern analysis (MVPA)
Psychophysiological interactions

ABSTRACT

Human neuroimaging studies indicate that the early visual cortex (EVC), including the primary visual cortex (V1), is involved in haptic exploration of objects, even when visual information is not available. However, it remains unknown whether the features of haptically explored objects, like size, are represented in the EVC. Here, we investigated whether we can use the activity patterns in the EVC and other task-relevant brain regions to decode stimulus size during haptic exploration, and whether this effect is due to visual imagery. Twenty-five right-handed participants haptically explored or imagined the size of three rings (small, medium, large) in a slow-event-related fMRI study. Participants were blindfolded during the training and fMRI sessions. Using multivariate pattern analysis, we found that V1 and the occipital pole (OP) showed accurate decoding of stimulus size during haptic exploration, but not imagery trials. This suggests that the activity patterns observed in the haptic condition cannot be explained by visual imagery. Frontal and parietal regions, as well as the multisensory lateral occipital tactile-visual area (LOtv), showed accurate size decoding during both haptic and imagery conditions, suggesting a flexible representation of stimulus size that adapts to task demands. In addition, stimulus size could be decoded across tasks in the anterior and posterior intraparietal sulcus (aIPS, pIPS), and dorsal premotor cortex (dPM). Psychophysiological interaction analysis indicated that V1 and OP showed stronger functional connectivity with ventral and dorsal visual stream areas during the haptic as compared to the imagery task. Overall, stimulus size information is similarly represented in frontal and parietal cortices across haptic exploration and imagery, but not in early visual areas, demonstrating that only regions specialized for haptic exploration and imagery support generalized size representations.

1. Introduction

To make sense of the outside world, our brain constantly processes and filters incoming sensory information. Although our understanding of how this occurs in the visual domain has advanced considerably, much remains to be learned about the neural mechanisms that enable object recognition when sensory information is gained solely through haptics (i.e., active touch).

Existing studies suggest that brain areas commonly associated with visual processing are also recruited for processing tactile information (for reviews, see Lacey and Sathian, 2014; Sathian, 2016). However, it is still unclear the extent to which early visual areas respond to haptic object signals in the absence of visual information. For instance, the specific role they play and whether this role might be related to visual imagery, still need to be thoroughly investigated. A major source of evidence for the involvement of the visual cortex in tactile processing comes from research on blind individuals, which has shown that the early visual cortex (EVC) is engaged in tactile tasks such as Braille reading and tactile discrimination (Sadato et al., 1998). These findings can be explained by neuroplastic changes induced by the absence of visual input (Silva et al., 2018). Yet, they might also reflect a broader functional organization of visual areas that is shared by both blind and sighted individuals.

Studies of haptic object exploration in sighted participants have

* Corresponding author at: Center for Mind/Brain Sciences (CIMeC), University of Trento, Piazza Manifattura 1, edificio 14, 38068 Rovereto (TN), Italy.
E-mail address: simona.monaco@unitn.it (S. Monaco).

https://doi.org/10.1016/j.neuroimage.2026.121774
Received 30 June 2025; Received in revised form 15 December 2025; Accepted 3 February 2026
Available online 4 February 2026

provided evidence for EVC activation during haptic exploration of objects in the absence of online visual input (Merabet et al., 2007; Monaco et al., 2017; Singhal et al., 2013; Snow et al., 2014). These findings suggest that, even with an intact visual system, haptic exploration of unseen stimuli recruits the EVC. However, the specific aspects of haptic exploration that elicit this activity remain unclear. The cross-modal influence of visual areas could be driven by at least two non-mutually exclusive neural mechanisms. First, somatosensory and motor signals elicited during haptic exploration might convey information about object properties, like size and shape, to the EVC via feedback connections. Second, activation in the EVC could result from visual imagery elicited during haptic exploration, which might facilitate the mental reconstruction of the explored object. Exploring the relative contributions of these mechanisms is crucial in order to understand whether and how the EVC supports the representation of object-related properties across sensory modalities and task demands.

In the present study, we focused on a specific object feature, namely size, because it can be rigorously controlled within the experimental setting. Specifically, we systematically varied object size while keeping other features (e.g., shape) constant. By using circular stimuli of different sizes, we ensured that the explored dimension remained consistent regardless of how the stimulus was explored.

In doing so, we aimed to determine the neural mechanisms underlying haptic stimulus size processing, and whether the haptic and visual imagery systems share the same size representation. Specifically, we pursued two main goals using functional magnetic resonance imaging (fMRI). First, we investigated whether the size of visually imagined and haptically explored, unseen stimuli can be decoded from activity patterns in early visual areas, including the primary visual cortex (V1) and the occipital pole (OP), which corresponds to central vision. Accurate decoding of haptic size in EVC would indicate that EVC processes size information acquired through the motor and haptic system, either via feed-back mechanisms, or indirectly via visual imagery. Further, if size can be accurately decoded during haptic exploration, but not visual imagery, this would argue against the visual imagery hypothesis. Second, we tested whether an abstract representation of size is shared across haptic exploration and visual imagery. If V1 and OP have such a task-independent representation of size, this would support the hypothesis of a more abstract coding mechanism that is not strictly tied to task demands. Importantly, we examined these size representations not only in early visual areas but also in regions of the frontal and parietal cortices known for their roles in action planning, execution, and imagery, as well as in lateral occipital and temporal areas involved in visual object recognition. Indeed, these areas may encode object properties, like size, that are relevant for action and/or object recognition, and thus, influence the activity of early visual areas through feedback connections. For example, it is well established that frontal and parietal regions are involved in hand movements and action plans (Filimon, 2010; Gallivan and Culham, 2015). Specifically, parietal regions, like the anterior intraparietal area (aIPS), play a role in computing object properties such as size for the selection of appropriate hand configurations to enable accurate hand-object interactions (Cavina-Pratesi et al., 2007; Monaco et al., 2014). Meanwhile, occipito-temporal regions contain high-dimensional object representations, and as such, they contribute to the recognition of object identity and category, as well as to semantic processing (for a review, see Bracci and Op de Beeck, 2023).

To achieve our aims, we blindfolded our participants and asked them to either haptically explore or visually imagine the size of three, concentric rings engraved on a plastic surface. During both the Haptic exploration and Visual imagery tasks, we acquired participants' fMRI data and applied multivoxel pattern analysis (MVPA) to examine the representational content associated with each ring size. Specifically, we tested whether a classifier could accurately discriminate between the three stimulus sizes based on voxel activity patterns in EVC and higher-level cortical areas during Haptic exploration, Visual imagery, and across the two tasks. By analyzing decoding accuracies for Haptic exploration and Visual imagery separately, we could test whether early visual areas and other brain regions encode size consistently within each task. In addition, the performance of the classifier trained on Haptic exploration and tested on Visual imagery, and vice versa, informed us about the existence of abstract representations of size shared across conditions, regardless of whether size was haptically explored or visually imagined. Significant cross-decoding accuracy would suggest that similar neural mechanisms underlie the processing of stimulus size in both the Haptic and Visual imagery tasks. In contrast, distinct activation patterns would indicate specialized neural representations specific to each task.

2. Materials and methods

2.1. Participants

Twenty-five participants were recruited for this study (13 females; age: $M = 25.11$, SD $= 3.98$). Participants were all right-handed, had normal or corrected-to-normal vision, and no history of neurological or psychiatric disorders. This research adhered to the guidelines outlined in the Declaration of Helsinki. The Human Research Ethics Committee of the University of Trento approved the experimental protocol of this study (protocol 2021–040). All participants provided written informed consent to participate in the experiment and received a monetary reimbursement for their participation.

2.2. Experimental design and paradigm

We used a slow event-related fMRI design to measure the blood-oxygenation-level dependent (BOLD) signal (Ogawa et al., 1992) while participants performed Haptic exploration and Visual imagery tasks. The two tasks consisted of haptically exploring one of three differently sized rings with the right (dominant) hand or visually imagining them. Therefore, we had a 2 × 3 repeated measures design (Fig. 1A) with factors: "task" (Haptic exploration vs. Visual imagery) and "size" (Small, Medium, and Large). This design resulted in six conditions: Touch Small, Touch Medium, Touch Large, Imagine Small, Imagine Medium, and Imagine Large. Importantly, participants were blindfolded throughout the entire experiment and had not seen the stimuli prior to the experimental session, which included a training phase followed by fMRI data acquisition.

At the beginning of the experiment, participants rested their right hand with the index finger and thumb placed together at the centre of a tablet, in correspondence of a small groove that served as a reference point for the resting position. Each trial started with an auditory instruction indicating the task to be performed (Touch or Imagine) and the size of the target circle (Small, Medium, or Large) (Fig. 1B). After 6 s, a "Stop" sound instructed participants to either stop exploring the circle and return their fingers to the resting position (Haptic trials), or to stop imagining the circle (Visual imagery trials). The "Stop" instruction served two main purposes: (1) to ensure that Haptic and Visual imagery trials had similar durations, and (2) to maintain a consistent return-phase duration across different movement types, thereby preventing potential differences in brain activation from being attributed to variations in Haptic task duration. The next trial started after 12 s of inter-trial interval (ITI). This ITI duration enabled the fMRI response to return to baseline before the onset of the next trial, thus avoiding contamination of the BOLD signal in the subsequent trial (e.g., Gallivan et al., 2011; Monaco et al., 2019; Singhal et al., 2013). During the ITI and imagery trials, participants kept their hand in the resting position.

To instruct participants about the size of the target circle to be explored, we used three letters (J, P, and Q) to be associated with the three stimulus sizes (e.g., Small = *P*, Medium = *J*, Large = *Q*). Therefore, the auditory cues consisted of: "Touch J", "Touch P", "Touch Q", "Imagine J", "Imagine P", and "Imagine Q". This weakened the possible influence of quantitative information about spatial magnitude that the

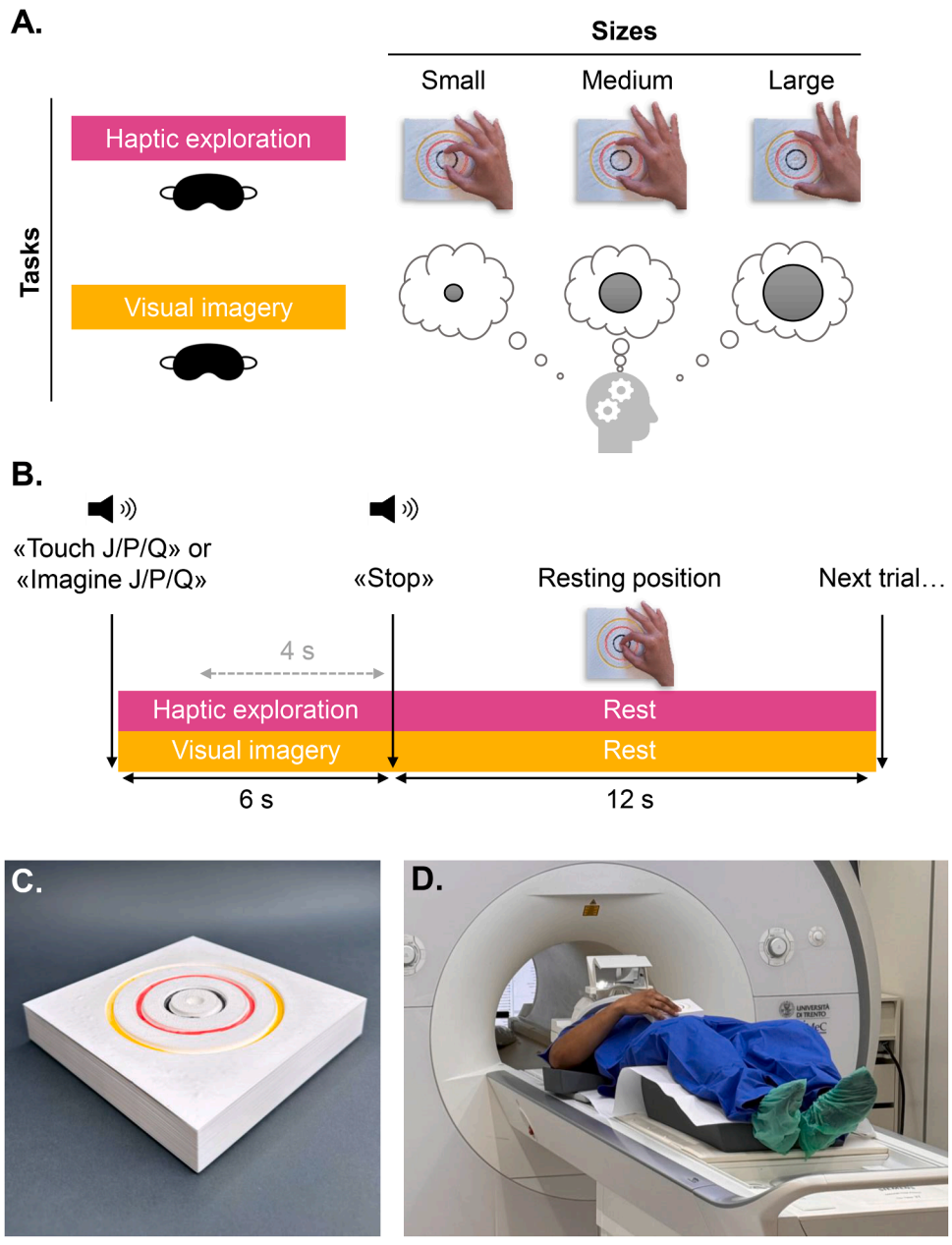

Fig. 1. Experimental design, paradigm, stimulus and setup. A. We employed a 2 × 3 repeated-measures design with three ring sizes (Small, Medium, and Large) and two tasks (Haptic exploration and Visual imagery) as factors. Participants were blindfolded during the training and experimental sessions. **B.** At the beginning of each trial, a recorded voice instructed participants about the task that they had to perform, which was to either haptically explore or visually imagine one of the three stimulus sizes. Participants performed the task for 6 s; after that, a "stop" cue prompted participants to stop performing the task, and to return the hand to the resting position when performing Haptic exploration trials. We used an inter-trial interval (ITI) of 12 s. We performed the analysis on the last 4 s of the 6 s task phase as indicated by the dashed grey line. **C.** The experimental stimulus consisted of a three-dimensional (3D) plastic tablet with three concentric circular rings of different sizes engraved on its surface. The grooves had diameters of 3 cm, 6.5 cm, and 10 cm, respectively. We marked the grooved with different colors to facilitate the distinction between the three differently sized rings from in the video recordings. **D.** The setup required participants to lay supine with the stimulus placed on their abdomen. The right upper arm was supported with foam, while the left arm rested beside the body.

words "small", "medium", and "large" clearly convey (e.g., Moretto and di Pellegrino, 2008). We identified all the nine possible associations between the three letters and the three object sizes and we randomly assigned them to our participants. Prior to the scanning session, each participant underwent a short training session (10–15 min) to learn the predefined letter-size associations and become familiar with the two tasks. All auditory cues were created using a freely available voice synthesizer (https://voicemaker.in/).

Participants were asked to keep their eyes closed and wore an eye-mask throughout the training and scanning sessions to prevent visual processing of the stimulus and the workspace. Therefore, they never saw the stimulus, neither before, nor during the experiment. Since participants had no prior visual experience of the stimuli, the initial trials of the training session were always Haptic trials. For the subsequent Visual imagery trials, participants were instructed to use the previously acquired haptic information to calibrate the mental visual images of the three stimulus sizes. As such, the Visual imagery task relied exclusively on information acquired through haptic exploration. In Haptic trials, participants were asked to use their thumb and index finger to haptically explore the target ring by performing circular movements along the

corresponding groove on the tablet.

A video camera placed in the magnet room recorded participants' hand movements during the experiment for off-line analysis of errors. Errors included incorrect task execution, such as exploring more than one groove within a single trial due to mislocalization of the target groove or unintentionally performing an action during a Visual imagery trial. These trials were excluded from further analysis, resulting in the removal of 3.6 % of trials in total from the dataset. To help the experimenter distinguish between the three differently sized rings in the video recordings, the grooves were marked with distinct colours (small groove: black; medium groove: red; large groove: yellow; Fig. 1C).

Each run lasted approximately nine minutes and included five trials for each of the six experimental conditions, for a total of 30 trials per run. The order of the six conditions was pseudorandomized within each run and counterbalanced across all runs so that each trial type was preceded and followed equally often by other trial types across the experiment. Participants completed six functional runs for a total of 180 trials per subject (30 trials per condition). One participant was excluded from the analyses due to technical issues that prevented complete data acquisition.

2.3. Stimuli and apparatus

We used a real and tangible three-dimensional (3D) stimulus that consisted of a plastic tablet featuring three concentric circular rings engraved on its surface (Fig. 1C). We selected rings in the form of grooves because they can be reliably explored for size while retaining a consistent shape, texture, and weight across conditions. The grooves had diameters of 3 cm, 6.5 cm, and 10 cm, respectively. The stimulus was designed with Autodesk Fusion 360 and printed on a 3D printer (Ulti-Maker 2+ Connect). While lying on the magnetic resonance (MR) bed, participants had the tablet placed on their abdomen (Fig. 1D); the tablet was attached with Velcro to a belt worn by the participants during the experiment. The position of the tablet could be adjusted to ensure that each participant could comfortably and naturally explore the stimulus. The right upper arm of the participants was supported with foam, and the left arm rested beside the body. Auditory cues were played through ePrime software, which was triggered by a computer that received a signal from the magnetic resonance imaging (MRI) scanner.

2.4. MRI parameters

The study was conducted at the Center for Mind/Brain Sciences (University of Trento, Italy) using a 3-T SIEMENS MAGNETOM Prisma MRI system with a 64-channel head coil. Functional images were acquired with a T2*-weighted segmented gradient echo-planar imaging sequence (Repetition time (TR) 2 s; Echo time (TE) 28 ms; Flip angle (FA) 75 deg; Field of view (FOV): 200 × 200 mm; in-slice resolution of 2 × 2 mm; slice thickness: 2 mm; multiband slice acceleration: 3). Each volume comprised 69 slices acquired in ascending interleaved order. At the beginning of each experimental session, a T1-weighted anatomical reference volume was acquired using a MPRAGE sequence (TR: 2530 ms; Inversion time (TI): 1100 ms; FA: 7 deg; FOV: 256 mm; 176 slices; 1 mm isotropic voxel resolution).

2.5. fMRI data pre-processing

We analysed the imaging data using Brain Voyager QX 2.8.4 (Brain Innovation, Maastricht, The Netherlands). Functional data were superimposed on anatomical brain images, aligned with the anterior commissure–posterior commissure line, and transformed into Talairach space (Talairach and Tournoux, 1988).

Functional data were pre-processed with temporal smoothing to remove frequencies below 2 cycles per run. We applied slice-time correction with a cubic spline interpolation algorithm. Each functional run was motion-corrected using a trilinear/sinc interpolation algorithm, such that each volume was aligned to the volume of the functional scan closest to the anatomical scan. The motion correction parameters of each run were also checked. Functional data from each run were screened to ensure that no obvious motion artifacts (e.g., rims of activation) were present in the activation maps of individual participants. For univariate analysis, we applied spatial smoothing using a Gaussian kernel with an 8-mm full width at half maximum. In contrast, no spatial smoothing was applied for multivariate analysis.

2.6. Univariate analysis

We used univariate analysis to localize areas that are well known to be involved in haptic and imagery tasks. To do so, we defined a general linear model (GLM) including seven predictors for each participant. The predictors were: (1) Touch Small, (2) Touch Medium, (3) Touch Large, (4) Imagine Small, (5) Imagine Medium, (6) Imagine Large, (7) Audio instruction. We also included six motion parameters (3 rotations and 3 translations) and error trials, if present, as predictors of no interest. The estimated beta weight (β) for each condition was converted to percent signal change; therefore, β values were scaled with respect to the mean signal level, and a random-effects (RFX) analysis was performed at the group level. We applied cluster-level correction (Forman et al., 1995) using the Brain Voyager's cluster-level statistical threshold estimator plug-in (Goebel et al., 2006), which implements Monte Carlo simulations (1000 iterations). Only foci that survived cluster threshold correction at an alpha-correction level of 0.01 are shown.

We created the average cortical surface using the anatomical images of 20 participants with cortex segmentation and cortex-based alignment procedures as implemented in Brain Voyager. Statistical activation maps were then projected onto the average surface map.

We performed a univariate conjunction analysis of Haptic exploration and Visual imagery (Haptic exploration AND Visual imagery). The conjunction analysis showed the recruitment of a widespread cluster of regions on both left and right hemispheres, including prefrontal, parietal, superior temporal, and occipital cortices (Fig. 2). We used the activation map of the conjunction analysis to functionally localize areas that showed above baseline activation for Haptic and Visual imagery trials. This allowed us to select areas involved in both tasks while also avoiding biases towards either task. The main focus of the study was to examine whether the activity pattern in the EVC can be used to decode the size of haptically explored stimuli and eventually exclude the potential role of visual imagery. Therefore, the selection criterion used to functionally localize our regions of interest (Haptic exploration AND Visual imagery) was independent from the key comparison explored in further analyses (Small vs. Medium, Medium vs. Large, and Small vs. Large stimulus size), ensuring no bias towards our predictions (Kriegeskorte et al., 2010; Vul and Kanwisher, 2010).

2.7. Regions of interest

The main objective of this study was to investigate whether 1) imagined and haptically explored size of unseen stimuli can be decoded from fMRI activity patterns, especially in early visual areas including V1 and the foveal cortex in OP, and whether 2) this representation, if present, is shared across haptic exploration and visual imagery. To this end, we localized areas V1 and OP, as well as specific ROIs in the dorsal and ventral visual streams, known for their involvement in movement execution, visual imagery, and object recognition. In particular, we explored the role of haptic exploration and visual imagery in 11 cortical regions in the left and right hemisphere, including areas that are known to support specific functions like visual information processing (i.e., V1, OP, inferior temporal cortex), visuo-tactile information processing (i.e., lateral-occipital tactile-visual area; LOtv), action execution and somatosensory processing (i.e., primary motor and somatosensory cortex), action planning, preparation and monitoring (i.e., supplementary and pre-supplementary motor area, dorsal and ventral premotor area) and

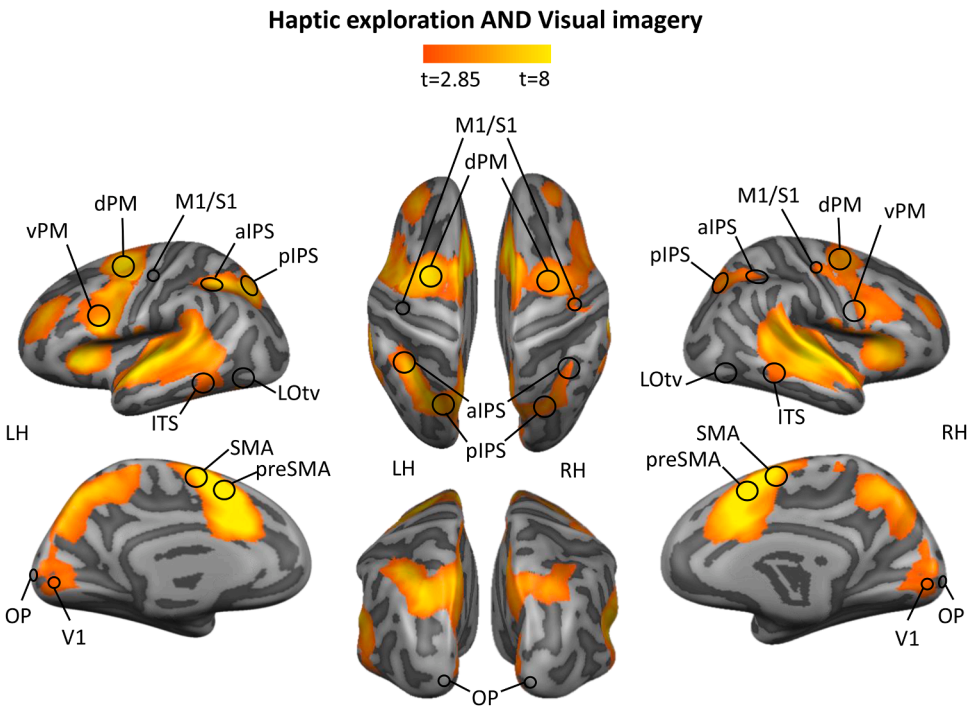

Fig. 2. Conjunction analysis of Haptic exploration and Visual imagery, and group ROIs. The figure shows the voxelwise statistical map obtained from the Haptic and Visual imagery univariate conjunction analysis. The group activation map is overlaid on the average cortical surface derived from the cortex-based alignment performed on 20 participants. Overlaid on the statistical map are regions of interest (ROIs) selected bilaterally for multivoxel pattern analysis (MVPA), including the primary motor/somatosensory area (M1/S1), dorsal and ventral premotor areas (dPM and vPM), supplementary and presupplementary motor areas (SMA and preSMA), anterior and posterior intraparietal sulci (aIPS and pIPS), inferior temporal sulcus (ITS), lateral-occipital tactile-visual area (LOtv), primary visual cortex (V1), occipital pole (OP).

coding of movement intention along with motor imagery processes (anterior and posterior intraparietal sulcus).

We localized our ROIs based on functional and anatomical methods. For functional localization, we used the group-level conjunction map of the RFX-GLM (Haptic exploration AND Visual imagery, $p < 0.01$) and searched for significant activation that coincided with the expected anatomical location. We used the same threshold for all ROIs. The activation map was corrected for multiple comparisons using the Monte Carlo simulation approach implemented in the BrainVoyager's cluster threshold plug-in (Forman et al., 1995; Goebel et al., 2006). We used an alpha-correction level of 0.01. Only foci that survived cluster threshold correction are shown in Fig. 2. When the univariate conjunction analysis did not reveal significant activation around one of our regions of interest (e.g., left M1/S1, bilateral OP and LOtv), we localized the area based on group-level anatomical landmarks and Talairach coordinates reported in previous studies. Talairach (TAL) coordinates of our ROIs are listed in Table 1 and illustrated in Fig. 2.

We defined our ROIs with region-specific radii optimized for anatomical and functional considerations. For early sensory and primary motor regions—specifically V1, OP, and primary motor/somatosensory cortex (M1/S1)—we used a 6-mm radius (925 mm^3) for each ROI. We reasoned that, since these areas are known for their high functional specificity and consistent anatomical landmarks, a small ROI would reliably capture the core activity without incorporating adjacent, functionally distinct areas. For regions that show greater spatial heterogeneity and less sharply defined boundaries (e.g., higher-order visual, multisensory, and association areas), we used a larger, 9-mm radius (3071 mm^3). This radius ensures adequate coverage of the distributed and potentially variable functional representations observed in higher-order regions and across individuals.

We identified seven bilateral ROIs in frontal and parietal lobes known for their role in action planning and execution (Gallivan et al., 2011), as well as in motor imagery (Hardwick et al., 2018). As shown in Fig. 2, the dorsal premotor cortex (dPM) was located at the intersection

Table 1
ROIs Talairach coordinates.

ROI	Coordinates (Talairach)		
	x	y	z
Left preSMA	−9	9	52
Right preSMA	9	9	52
Left SMA	−9	−9	58
Right SMA	9	−9	58
Left dPM	−27	−6	53
Right dPM	27	−10	55
Left vPM	−54	8	28
Right vPM	54	8	28
Left M1S1*	−39	−20	52
Right M1S1	41	−16	50
Left aIPS	−38	−48	45
Right aIPS	32	−43	40
Left pIPS	−17	−68	43
Right pIPS	22	−64	40
Left OP*	−11	−96	1
Right OP*	12	−96	1
Left V1	−9	−83	0
Right V1	9	−83	1
Left LOtv*	−48	−62	−7
Right LOtv*	48	−60	−6
Left ITS	−55	−44	−7
Right ITS	56	−42	−7

Note: all ROIs have the same number of anatomical voxels (3071 mm^3; ROI radius of 9 mm), except for bilateral M1S1, V1, and OP (925 mm^3; ROI radius of 6 mm). Asterisks (*) indicate the ROIs localized based on group-level anatomical landmarks and Talairach coordinates reported in previous studies. The remaining ROIs were defined by the intersection of the group-level conjunction map of the RFX-GLM (Haptic exploration AND Visual imagery) and their expected anatomical locations.

of the superior frontal sulcus and the precentral sulcus (Monaco et al., 2014). The primary motor/somatosensory cortex (M1/S1) was defined by selecting voxels in the fundus of the central sulcus and spanning pre- and post-central gyri at the omega-shaped hand knob. The ventral premotor cortex (vPM) was identified by selecting voxels slightly below and behind the junction of the inferior frontal sulcus and precentral sulcus (Gallivan et al., 2011). The supplementary motor area (SMA) was identified at the junction of the superior frontal gyrus and the cingulate gyrus, while the pre-supplementary motor area (preSMA) was located more anteriorly compared to SMA. The anterior intraparietal sulcus (aIPS) was selected at the intersection of the intraparietal sulcus and the inferior segment of the postcentral sulcus (Culham et al., 2003), while the posterior intraparietal sulcus (pIPS) was located more posteriorly along the intraparietal sulcus compared to the aIPS.

We also identified four bilateral ROIs in occipital and temporal lobes known for their specialization in visual and multisensory processing, as well as object recognition. In particular, V1 was located in the calcarine sulcus, while the OP was localized at the most posterior region of the occipital lobe, corresponding to the caudal end of the calcarine sulcus. The LOtv was mapped to the junction of the ascending limb of the inferior temporal gyrus and the lateral occipital sulcus (Amedi et al., 2001). Finally, the inferior temporal sulcus (ITS) was localized at the inferior aspect of the temporal lobe.

2.8. Multivoxel pattern analysis

To perform MVPA, we employed a Linear Discriminant Analysis (LDA) classifier using the CoSMoMVPA Toolbox (Oosterhof et al., 2016). For each participant and each of the 22 ROIs, β weights were estimated from non-spatially smoothed data using the design matrix specified in the GLM. Activity patterns were decoded from individual runs, and classification accuracy was assessed using a 'leave-one-run-out' cross-validation approach. Since the classifier requires at least two samples per class for the training, and error trials were excluded, we had to discard some functional runs (5 runs across 3 participants) from the MVPA due to an insufficient number of trials for the training phase. Thus, a new GLM was estimated for these participants, excluding the above-mentioned runs to satisfy the requirements of the CoSMoMVPA Toolbox.

MVPA was conducted using both ROI-based and whole-brain searchlight approaches (Kriegeskorte and Bandettini, 2007), performing decoding analysis across all voxels in the brain. The searchlight analysis served to replicate and potentially extend the ROI-based results, though its spatial specificity is inherently limited, as decoding results for each searchlight are assigned to its central voxel (Oosterhof et al., 2011). Each searchlight was defined using the beta values of the selected voxel and its surrounding neighbours within a sphere of three-voxel radius, averaging 123 anatomical voxels per searchlight.

To investigate whether the haptically explored and imagined size of stimuli could be decoded from activity patterns in our ROIs, we trained the classifier to discriminate between two sizes within each of the three stimulus size pairs, separately for Haptic trials (Touch Small vs. Touch Medium, Touch Medium vs. Touch Large, and Touch Small vs. Touch Large) and Visual imagery trials (Imagine Small vs. Imagine Medium, Imagine Medium vs Imagine Large, and Imagine Small vs. Imagine Large). Classification accuracies were then averaged to obtain a mean accuracy for each ROI. To assess whether the representation of stimulus size, if present, is shared across Haptic exploration and Visual imagery, we performed cross-decoding. Specifically, we trained the classifier on the distinction between two sizes within each of the three pairs of sizes in Haptic trials (e.g., Touch Small vs. Touch Medium) and tested its performance to distinguish between the same size pairs in Visual imagery trials (e.g., Imagined Small vs. Imagined Medium), and vice-versa. Classification accuracies for the cross-decoding of the three comparisons were also averaged.

For ROI-based MVPA, we evaluated the statistical significance of mean classification accuracies using a two-tailed, one-sample *t*-test against chance-level decoding (50 %) for each ROI. To account for multiple comparisons (22 ROIs × 3 comparisons), statistical results were corrected using the False Discovery Rate (FDR) method (Benjamini and Hochberg, 1995). To test for significant differences in the mean decoding accuracies between Haptic exploration, Visual imagery, and Cross-decoding conditions, we also performed a two-tailed, paired sample *t*-test between each pair of decoding type (e.g., Haptic size decoding vs. Visual imagery size decoding, Haptic size decoding vs. Cross-decoding, Visual imagery size decoding vs. Cross-decoding), for each ROI. Statistical results were corrected for multiple comparisons using the FDR procedure. The rationale for these comparisons is as follows: comparing Haptic vs. Visual imagery size decoding allows us to assess whether size information is more accurately discriminated in one task than the other within a given ROI. Comparisons between Haptic size vs. Cross-decoding, and Visual imagery size vs. Cross-decoding, inform us about whether the abstract representation of size, reflected in the Cross-decoding, differs from either the haptic or imagined representation. For instance, above-chance Cross-decoding but lower accuracy than within-task modality decoding would indicate that an abstract size representation exists, but that one task modality (the one with higher decoding accuracy) provides a more precise representation than the abstract one. Conversely, above-chance Cross-decoding with no difference with Haptic or Visual imagery decoding would suggest that a region contains an abstract representation of size that is independent of the task modality used to acquire it. A third possibility is that Cross-decoding is not significant, indicating that size representations in that region are task-specific. We do not expect Cross-decoding to exceed within-task modality decoding accuracy because generalizing across two different tasks typically results in a lower signal-to-noise ratio.

For searchlight-based MVPA, we identified brain areas where decoding exceeded chance level (50 %) by performing *t*-tests across individual decoding accuracy maps. Each resulting map corresponds to the average of the individual comparisons (Small vs. Medium, etc. for Haptic, Visual imagery trials, and Cross-decoding). As for the univariate analysis, statistical maps were corrected for multiple comparisons using the Brain Voyager's cluster-level statistical threshold estimator plug-in (Forman et al., 1995; Goebel et al., 2006), which implements Monte Carlo simulations (1000 iterations). Only foci that survived cluster threshold correction at an alpha-correction level of 0.05 for Visually imagined size decoding and Size cross-decoding searchlight statistical maps, and 0.001 for the Haptic size decoding searchlight statistical map are shown. We then projected the average statistical maps originating from the searchlight analysis onto the average surface map.

2.9. Psychophysiological interaction (PPI) analysis

We used the PPI method (Friston et al., 1997; McLaren et al., 2012; O'Reilly et al., 2012) to estimate the task-specific changes in functional connectivity between our seed regions (left OP and V1) and the rest of the brain during the Haptic versus Visual imagery task. PPI identifies brain regions in which functional connectivity is modified by the task above and beyond simple interregional correlations ("physiological component") and task-modulated activity ("psychological component"). For each seed region, and for each run of each participant, we created a PPI model that included the following: (1) the physiological component, corresponding to the *z*-normalized time course extracted from the seed region; (2) the psychological component, corresponding to the task model (boxcar predictors convolved with a standard hemodynamic response function); and (3) the PPI component, corresponding to the *z*-normalized time course multiplied, volume by volume, with the task model. The boxcar predictors of the psychological component were set to 1 for the Haptic task, to −1 for the Visual imagery task, and to 0 for baseline. Motion correction parameters from each run of each participant were included as co-variates of no interest. The individual GLM design matrix files were used for a random-effects model analysis

(Friston et al., 1999). The functional connectivity map was corrected for multiple comparisons using the Monte Carlo simulation approach implemented in the BrainVoyager's cluster threshold plug-in (Forman et al., 1995; Goebel et al., 2006). The minimum cluster sizes were 178 and 181 functional voxels for maps originated with left hemisphere (LH) OP and V1 as seed regions, respectively ($F = 2.2$; 1424 and 1448 mm^3). We used an alpha-correction level of 0.05.

2.10. Subjective vividness rating

The ability to generate vivid visual images varies significantly across individuals (Cui et al., 2007). We assessed the vividness of visual imagery in our participants to ensure they possessed a robust ability to form mental images. To do so, at the end of the experimental session, participants completed the Vividness of Visual Imagery Questionnaire (VVIQ), which evaluates the quality of their visual imagery (Marks, 1995). The questionnaire includes 16 items, each requiring participants to rate the vividness of their visual imagery for various scenarios (e.g., a shop, a person, the sky) on a scale from 1 (no image present) to 5 (perfectly clear and vivid image). The total score ranges from 16 to 80, with higher scores indicating higher vividness of visual imagery. We calculated the mean vividness score as an indicator of each participant's visual imagery ability.

To explore potential relationships between imagery vividness and neural activity, we computed Pearson's correlation coefficient (r) to measure the correlation between the vividness scores and classification accuracies in Visual imagery trials, Haptic trials, and in the Cross-decoding condition, separately, for each ROI. Importantly, the analysis of correlation for the Haptic and Cross-decoding conditions allowed us to examine whether individual differences in imagery vividness might be reflected in different neural mechanisms, and potentially different processing strategies, to represent haptic size and to generalize size information across the two tasks.

3. Results

3.1. ROI-based multivoxel pattern analysis

We performed MVPA in each ROI to test whether the size of unseen stimuli can be decoded from brain activity patterns during Haptic exploration, Visual imagery, and across Haptic and Visual imagery tasks. For each ROI, decoding accuracies and significant differences between each pair of decoding accuracies are shown in Figs. 3,4 and statistical values are reported in Tables 2,3. The statistical values of decoding accuracies for each of the three pairs of sizes are reported in Supplementary Table S1.

Nearly all ROIs in the occipital and temporal cortices, including the left V1, bilateral OP, LOtv, and ITS showed significant decoding accuracy of stimulus size during Haptic exploration (Fig. 3, magenta dots). In addition, the left LOtv showed above chance size decoding also during Visual imagery (yellow dots). Haptic size decoding was significantly higher than imagined size decoding in all occipital and temporal ROIs,

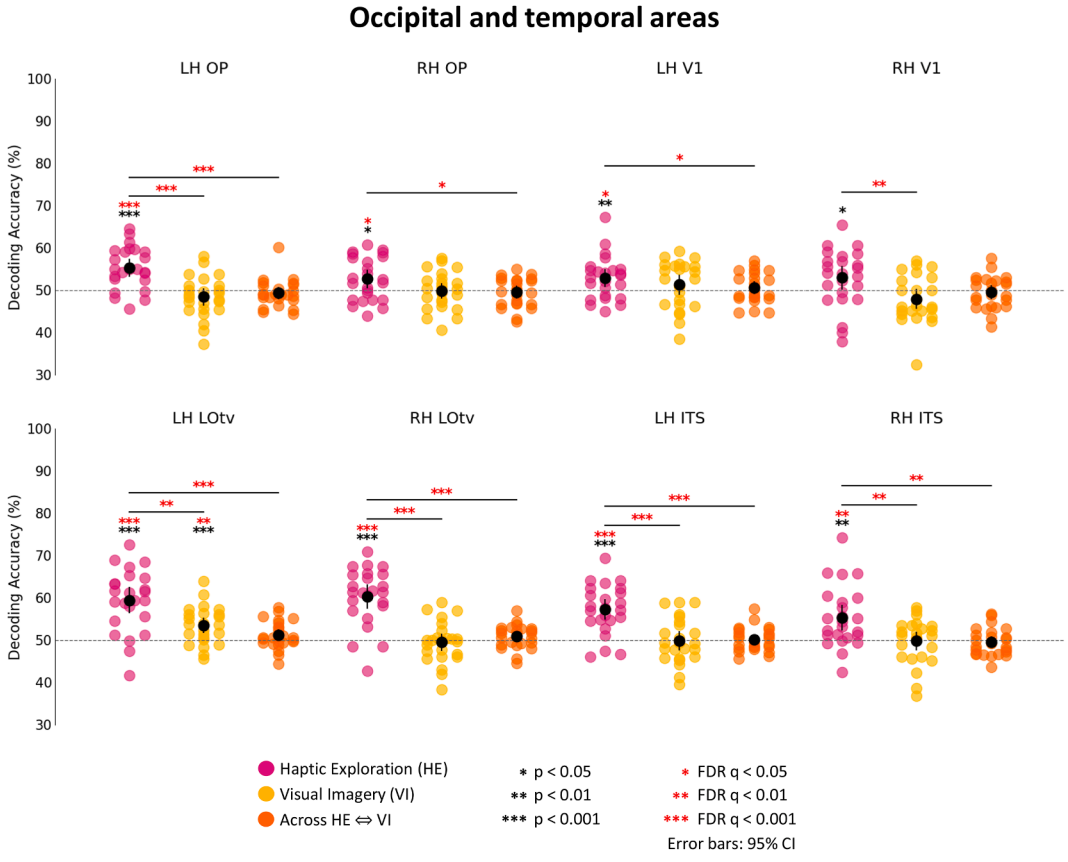

Fig. 3. Classifier decoding accuracies in occipital and temporal ROIs. The scatterplots show decoding accuracies for each participant along with the average (black circles) in occipital and temporal areas in both the left and right hemisphere for size information in Haptic Exploration (HE) trials (magenta circles), Visual Imagery (VI) trials (yellow circles), and across HE and VI (orange circles). Chance level is indicated with a line at 50% of decoding accuracy. Error bars represent 95% confidence intervals (CI). Asterisks (*) indicate statistical significance based on paired-samples, two-tailed *t*-tests across subjects with respect to 50%, and pairwise comparisons for each pair of decoding type (i.e., HE vs. VI, HE vs. Across HE and VI). Black asterisks denote uncorrected statistical significance, whereas red asterisks indicate statistical significance based on an FDR correction of $q < 0.05$. While all areas show significant above chance decoding accuracy of size information in HE trials, except for the right V1, in VI trials size information can only be decoded from the activity patterns of the left LOtv. In addition, no area shows significant above chance decoding accuracy of size information across HE and VI conditions.

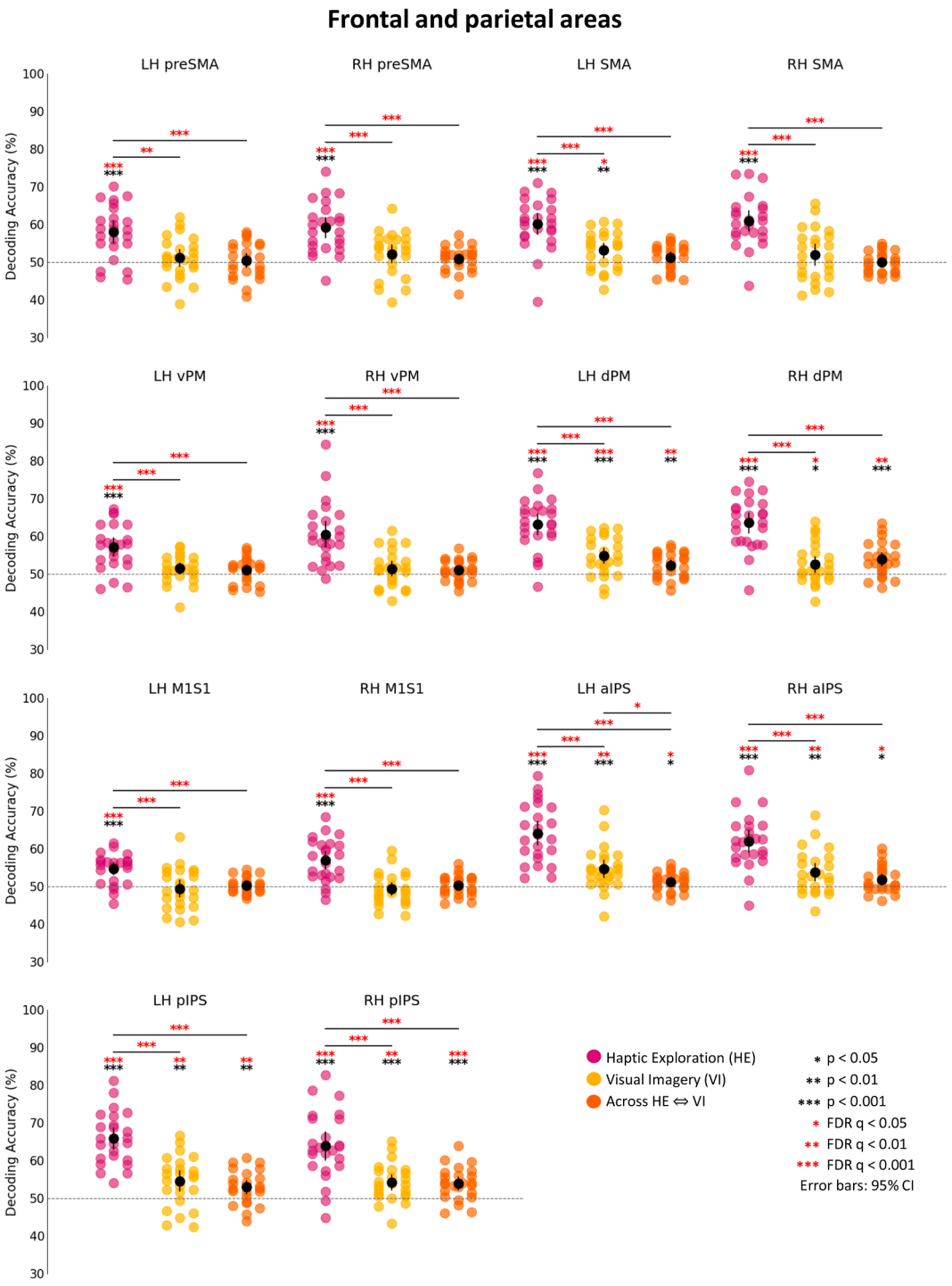

Fig. 4. Classifier decoding accuracies in frontal and parietal ROIs. The scatterplots show decoding accuracies for each participant along with the average (black circles) in frontal and parietal areas in both the left and right hemisphere for size information in Haptic Exploration (HE) trials (magenta circles), Visual Imagery (VI) trials (yellow circles), and across HE and VI (orange circles). Chance level is indicated with a line at 50% of decoding accuracy. Error bars represent 95% confidence intervals (CI). Asterisks (*) denote statistical significance based on paired-samples, two-tailed *t*-tests across subjects with respect to 50%, and pairwise comparisons for each pair of decoding type (i.e., HE vs. VI, HE vs. Across HE and VI, VI vs. Across HE and VI). Black asterisks indicate uncorrected statistical significance, whereas red asterisks indicate statistical significance based on an FDR correction of $q < 0.05$. While all areas show significant above chance decoding accuracy of size information in HE trials, in VI trials size information can only be decoded from the activity patterns of the left SMA, bilateral dPM area, bilateral aIPS, and pIPS. As for the decoding of size across HE and VI conditions, significant above chance accuracy is observed in bilateral dPM, aIPS, and pIPS.

except in the right OP and left V1. These results suggest that Haptic size decoding in visual areas (especially left OP and right V1) is not merely driven by visual imagery processes, as decoding was observed during Haptic exploration but not during Visual imagery alone, which is in contrast to what would be expected if the visual imagery hypothesis were true. In addition, the results suggest that LOtv contains distinct yet overlapping representations of haptically explored and imagined stimulus size. None of these areas showed significant decoding of size information across Haptic and Visual imagery tasks (orange dots), indicating that the representation of stimulus size does not generalize

Table 2
Statistical values for ROI-based MVPA results.

ROI	Decoding accuracy for size, t(23)		
	Haptic exploration	Visual imagery	Cross-decoding
Left preSMA	**$p<.001$ $t=5.60$**	$p=.311$ $t=1.04$	$p=.617$ $t=0.51$
Right preSMA	**$p<.001$ $t=6.70$**	$p=.082$ $t=1.82$	$p=.210$ $t=1.29$
Left SMA	**$p<.001$ $t=7.33$**	**$p=.005$ $t=3.11$**	$p=.076$ $t=1.86$
Right SMA	**$p<.001$ $t=7.98$**	$p=.185$ $t=1.37$	$p=.975$ $t=0.03$
Left dPM	**$p<.001$ $t=9.52$**	**$p<.001$ $t=4.65$**	**$p=.002$ $t=3.41$**
Right dPM	**$p<.001$ $t=9.95$**	**$p=.025$ $t=2.39$**	**$p<.001$ $t=4.23$**
Left vPM	**$p<.001$ $t=5.84$**	$p=.060$ $t=1.98$	$p=.109$ $t=1.67$
Right vPM	**$p<.001$ $t=6.21$**	$p=.164$ $t=1.44$	$p=.070$ $t=1.90$
Left M1S1	**$p<.001$ $t=5.76$**	$p=.634$ $t=-0.48$	$p=.477$ $t=0.72$
Right M1S1	**$p<.001$ $t=5.94$**	$p=.453$ $t=-0.76$	$p=.568$ $t=0.58$
Left aIPS	**$p<.001$ $t=8.84$**	**$p=.001$ $t=4.00$**	**$p=.024$ $t=2.42$**
Right aIPS	**$p<.001$ $t=8.07$**	**$p=.004$ $t=3.21$**	**$p=.018$ $t=2.55$**
Left pIPS	**$p<.001$ $t=11.18$**	**$p=.003$ $t=3.36$**	**$p=.003$ $t=3.30$**
Right pIPS	**$p<.001$ $t=7.49$**	**$p<.001$ $t=4.15$**	**$p<.001$ $t=4.46$**
Left OP	**$p<.001$ $t=5.25$**	$p=.134$ $t=-1.55$	$p=.328$ $t=-1.00$
Right OP	**$p=.018$ $t=2.56$**	$p=.853$ $t=-0.19$	$p=.525$ $t=-0.65$
Left V1	**$p=.010$ $t=2.81$**	$p=.248$ $t=1.19$	$p=.432$ $t=0.80$
Right V1	$p=.043$ $t=2.14$	$p=.086$ $t=-1.79$	$p=.543$ $t=-0.62$
Left LOtv	**$p<.001$ $t=6.29$**	**$p=.001$ $t=3.84$**	$p=.072$ $t=1.89$
Right LOtv	**$p<.001$ $t=7.42$**	$p=.619$ $t=-0.50$	$p=.143$ $t=1.52$
Left ITS	**$p<.001$ $t=6.13$**	$p=.923$ $t=-0.10$	$p=.729$ $t=0.35$
Right ITS	**$p=.001$ $t=3.65$**	$p=.841$ $t=-0.20$	$p=.478$ $t=-0.72$

Note: Statistically significant values after False Discovery Rate (FDR) correction ($q < 0.05$) for multiple comparisons are indicated in boldface.

Table 3
Statistical values for ROI-based MVPA results: pair-wise comparisons.

ROI	Decoding accuracy for size, t(23)		
	Haptic exploration vs. Visual imagery	Haptic exploration vs. Cross-decoding	Visual imagery vs. Cross-decoding
Left preSMA	**$p=.001$ $t=3.95$**	**$p<.001$ $t=4.76$**	$p=.658$ $t=0.45$
Right preSMA	**$p<.001$ $t=4.41$**	**$p<.001$ $t=6.11$**	$p=.301$ $t=1.06$
Left SMA	**$p<.001$ $t=4.86$**	**$p<.001$ $t=5.54$**	$p=.184$ $t=1.37$
Right SMA	**$p<.001$ $t=5.34$**	**$p<.001$ $t=7.42$**	$p=.205$ $t=1.30$
Left dPM	**$p<.001$ $t=6.12$**	**$p<.001$ $t=6.80$**	$p=.049$ $t=2.07$
Right dPM	**$p<.001$ $t=6.88$**	**$p<.001$ $t=6.12$**	$p=.241$ $t=-1.21$
Left vPM	**$p<.001$ $t=4.10$**	**$p<.001$ $t=4.64$**	$p=.715$ $t=0.37$
Right vPM	**$p<.001$ $t=4.38$**	**$p<.001$ $t=6.02$**	$p=.787$ $t=0.27$
Left M1S1	**$p<.001$ $t=4.15$**	**$p<.001$ $t=5.34$**	$p=.479$ $t=-0.72$
Right M1S1	**$p<.001$ $t=4.49$**	**$p<.001$ $t=4.88$**	$p=.289$ $t=-1.09$
Left aIPS	**$p<.001$ $t=4.81$**	**$p<.001$ $t=7.79$**	**$p=.007$ $t=2.93$**
Right aIPS	**$p<.001$ $t=4.96$**	**$p<.001$ $t=6.35$**	$p=.043$ $t=2.14$
Left pIPS	**$p<.001$ $t=6.53$**	**$p<.001$ $t=10.58$**	$p=.343$ $t=0.97$
Right pIPS	**$p<.001$ $t=5.06$**	**$p<.001$ $t=5.57$**	$p=.814$ $t=0.24$
Left OP	**$p<.001$ $t=4.94$**	**$p<.001$ $t=4.45$**	$p=.456$ $t=-0.76$
Right OP	$p=.075$ $t=1.86$	**$p=.014$ $t=2.65$**	$p=.800$ $t=0.26$
Left V1	$p=.325$ $t=1.00$	**$p=.031$ $t=2.30$**	$p=.581$ $t=0.56$
Right V1	**$p=.001$ $t=3.63$**	$p=.043$ $t=2.14$	$p=.222$ $t=-1.26$
Left LOtv	**$p=.005$ $t=3.11$**	**$p<.001$ $t=5.20$**	$p=.039$ $t=2.19$
Right LOtv	**$p<.001$ $t=6.74$**	**$p<.001$ $t=6.75$**	$p=.164$ $t=-1.44$
Left ITS	**$p<.001$ $t=4.47$**	**$p<.001$ $t=5.87$**	$p=.826$ $t=-0.22$
Right ITS	**$p=.002$ $t=3.42$**	**$p=.001$ $t=3.89$**	$p=.844$ $t=0.20$

Note: Statistically significant values after False Discovery Rate (FDR) correction ($q < 0.05$) for multiple comparisons are indicated in boldface.

across tasks in areas specialized in processing low-level visual features of objects (OP, V1) and object recognition (LOtv, ITS). All areas, except the right V1, showed higher accuracy for Haptic size than Cross-decoding.

As expected, the patterns of activity in all frontal and parietal ROIs enabled successful decoding of size during Haptic exploration (Fig. 4). These regions include bilateral preSMA, SMA, vPM, dPM, M1/S1, aIPS, and pIPS. Decoding of stimulus size during Visual imagery trials was significantly accurate in left SMA, bilateral dPM, aIPS, and pIPS. We also found higher decoding accuracy for Haptic than Visual imagery trials in parietal and frontal ROIs. Therefore, although these areas show a predominant role in haptic size processing, they can flexibly represent size information regardless of whether it is based on Haptic exploration or Visual imagery. Interestingly, bilateral dPM, aIPS, and pIPS also showed above-chance cross-decoding accuracy, suggesting that in these areas haptically explored and imagined size is represented using similar neural mechanisms. Moreover, we found higher decoding accuracy for Haptic size than Cross-decoding in frontal and parietal ROIs, and the left aIPS also showed higher decoding accuracy for Visually imagined size than Cross-decoding.

Taken together, these results suggest that both distinct and shared neural mechanisms underlie the representation of stimulus size during Haptic exploration and Visual imagery, with higher-order cortical areas flexibly representing size information across these tasks. In addition, the differential involvement of various brain regions highlights not only the complexity of processing stimulus-related features under different cognitive tasks, but also the role of both early visual and higher-order brain regions in encoding size information.

3.2. Searchlight-based MVPA

We complemented the ROI-based analysis with searchlight-based MVPA over the whole brain to identify brain regions where neural activity patterns reflected reliable decoding of the size during Haptic exploration, Visual imagery, and across the two tasks.

Overall, ROI-based and searchlight MVPA results were highly consistent. Specifically, for the Haptic condition, searchlight analysis revealed significant size decoding in widespread bilateral clusters encompassing frontal (including vPM, dPM, SMA, preSMA, and M1), parietal (including S1, aIPS, and pIPS), temporal (including ITS), and occipital regions (including lateral occipital cortex and OP), in both hemispheres (Fig. 5A). Although the calcarine sulcus did not show Haptic size decoding at the chosen threshold in the searchlight map, this information emerged at lower, yet still significant thresholds, consistent with the ROI analysis. Decoding of imagined size was significantly accurate in several clusters located in bilateral parietal cortices (including aIPS and pIPS), the left superior temporal cortex, bilateral lateral occipital cortices, while frontal decoding was markedly left-lateralized (including SMA and dPM) (Fig. 5B). Cross-decoding of size information yielded significant results in a large cluster spanning bilateral parietal cortices (including IPS), as well as additional clusters in bilateral frontal (including dPM areas), prefrontal, temporal, and superior occipital cortices (Fig. 5C).

3.3. PPI analysis

To summarize, our MVPA results show that the activity pattern from the patch of visual cortex corresponding to foveal vision (OP) and primary visual cortex (V1) can be used to decode stimulus size during Haptic exploration even if participants are blindfolded. These results might be due to feedback from high-level sensory-motor areas in the premotor cortex and intraparietal sulcus. To examine whether functional connectivity between left hemisphere OP and V1 and other regions (e.g., premotor and parietal areas) is modulated by the nature of the task, we used a PPI approach. When comparing Haptic with Visual imagery task, we found that the left OP and V1 (Fig. 6) showed stronger functional connectivity with several areas, including those implicated in sensory-motor control of grasping actions (left aIPS), multimodal recognition of objects (LOtv), somatosensory/motor function (premotor cortex). In particular, left OP (Fig. 6A) showed stronger connections for Haptic than Imagery tasks with left hemisphere cortical regions including aIPS, vPM, ITS, and LOtv. Similarly, left V1 (Fig. 6B) showed

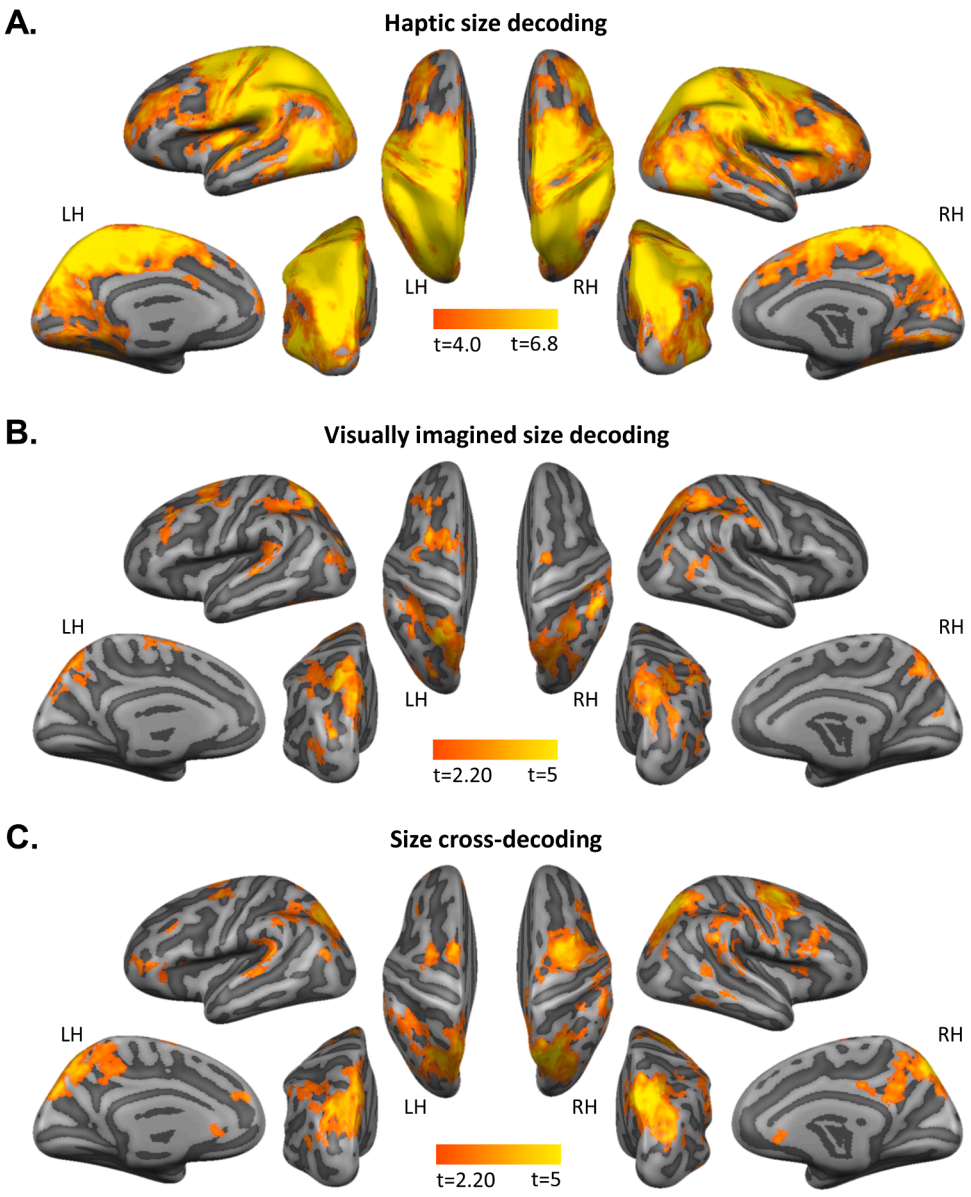

Fig. 5. Searchlight results for Haptic size, Visually imagined size, and Cross-decoding of size. A. The figure shows the decoding accuracy map for Haptic size which demonstrated a widespread cluster where decoding accuracies for haptically explored size were above chance-level. **B.** The figure shows the decoding accuracy map for Visually imagined size which revealed clusters in bilateral frontal cortices, bilateral parietal cortices, the left superior temporal cortex, and bilateral occipital cortices where decoding accuracies for visually imagined size were above chance-level. **C.** The figure shows the decoding accuracy map for the Cross-decoding of size which revealed clusters in bilateral prefrontal and frontal cortices, bilateral parietal cortices, the left superior temporal cortex, and bilateral occipital cortices where decoding accuracies for cross-decoding of size information were above chance-level. All maps are overlaid on the average cortical surface.

enhanced connectivity during Haptic exploration as compared to Visual imagery task with predominantly left-lateralized clusters, which include aIPS, pIPS, vPM, ITS, and LOtv. However, it is important to note that, for both PPI analyses, the results observed in parietal (aIPS, pIPS) and premotor (vPM) regions did not survive cluster-level correction. Together, the PPI results reinforce the suggestion that the OP and V1 play a role in haptic size exploration because of feedback connections from high-level sensory-motor areas.

3.4. Vividness of visual imagery

Overall, participants' performance in the VVIQ demonstrated average visual imagery ability (mean VVIQ score: 62.04; SD: 8.5; range: 47–75). Note that higher values indicate greater imagery vividness. We found a significant positive correlation between decoding accuracy in the Visual imagery condition and imagery vividness scores in left preSMA ($r_{(22)} = 0.43$, $p < 0.05$; Fig. 7A). None of the other ROIs showed a significant correlation. In addition, we found a significant negative correlation between VVIQ scores and decoding accuracy in the Haptic exploration condition in right M1/S1 ($r_{(22)} = -0.47$, $p < 0.05$; Fig. 7B). No significant correlation was found in the other ROIs. None of our ROIs showed a significant correlation between VVIQ scores and Cross-decoding accuracy. All Pearson's correlation coefficients (r) and statistical significance values are reported in Supplementary Table S2.

4. Discussion

Previous research has shown that haptic exploration of objects recruits early visual areas, despite the absence of concurrent visual input (Merabet et al., 2007; Monaco et al., 2017; Singhal et al., 2013; Snow et al., 2014). However, the specific aspects of haptic processing that drive this activation in EVC remain unclear. Here, we used MVPA to

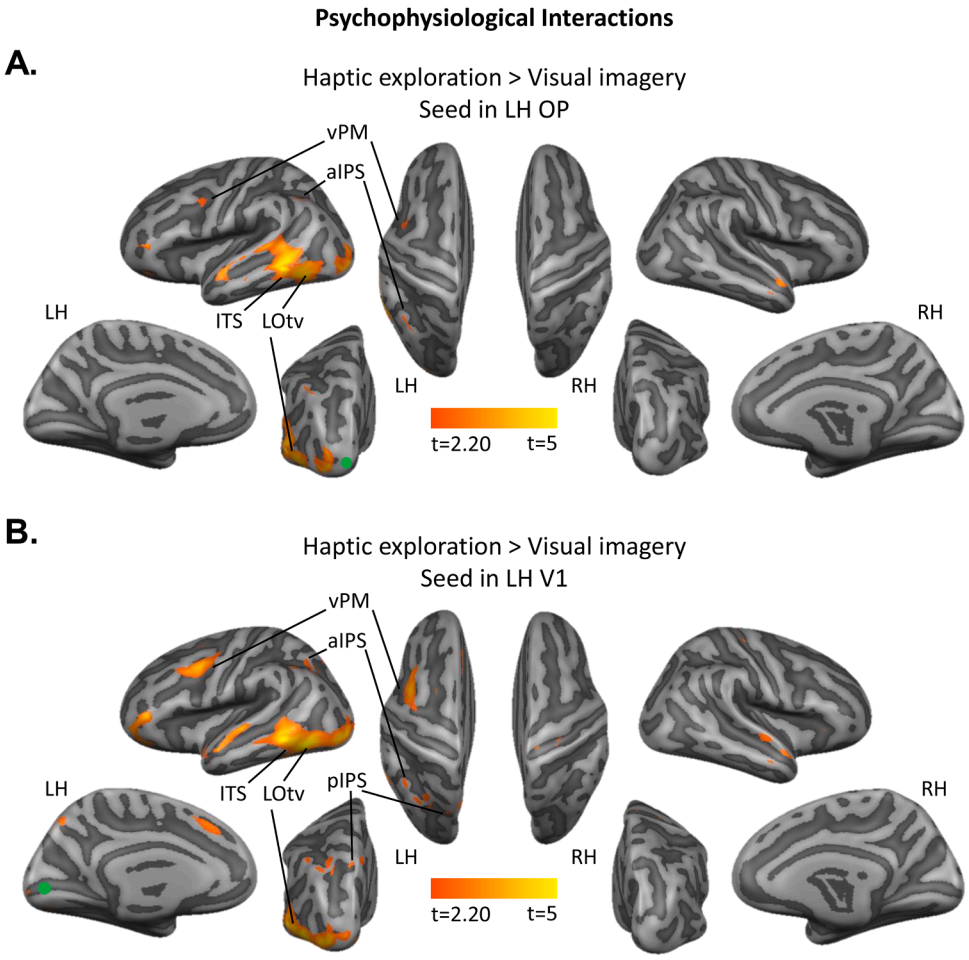

Fig. 6. Task-related functional connections between early visual areas and the rest of the brain. A. The figure shows the psychophysiological interaction results using left OP as seed region (green circle). The map indicates the brain areas that show stronger functional connections with left OP for Haptic exploration as compared to Visual imagery. The map is overlaid on the average cortical surface. **B.** The figure shows the psychophysiological interaction results using left V1 as seed region (green circle). The map indicates the brain areas that show stronger functional connections with left V1 for Haptic exploration as compared to Visual imagery. The map is overlaid on the average cortical surface.
Note: Results are shown at $p < 0.05$ uncorrected. Clusters in parietal (pIPS, aIPS) and premotor (vPM) cortices did not survive Cluster-threshold correction.

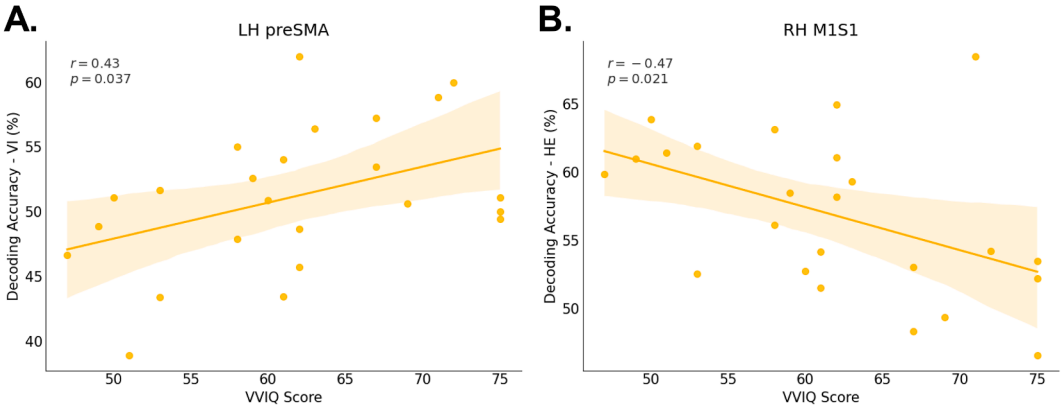

Fig. 7. Correlation between VVIQ scores and decoding accuracy (%). A. The scatterplot shows the correlation between the average decoding accuracy (%) for visually imagined size and the average VVIQ score of each participant, in left preSMA. **B.** The scatterplot shows the correlation between the average decoding accuracy (%) of haptically explored size and the average VVIQ score of each participant, in right M1S1. In both Panels, Pearson's correlation coefficient (r) and statistical significance are also shown on the top left. The translucent band around the regression line represents 95% confidence interval (CI). HE: Haptic Exploration; VI: Visual Imagery.

examine whether the dimension of haptically explored stimuli can be decoded based on the activity patterns in EVC, as well as in the action and perception networks. We also examined whether this effect could be related to visual imagery. Our results revealed that activity patterns in

occipito-temporal areas, including early visual areas such as OP and V1, as well as in frontal and parietal areas, allowed discriminating the sizes of haptically explored stimuli. Interestingly, the lack of imagined size decoding in the EVC suggests that the current findings are not driven by visual imagery. In contrast, haptically explored and visually imagined stimulus size could be decoded in LOtv, a multisensory area in the ventral visual stream, along with associative areas in frontal and parietal cortices, such as SMA, dPM, aIPS, and pIPS, suggesting that these regions flexibly represent size information based on task demands. We also performed cross-decoding to identify brain regions that potentially store a representation of size shared across the two tasks. This analysis yielded significant results in dPM, aIPS, and pIPS, indicating the existence of an abstract representation of size. Interestingly, in these areas haptic information still provides a more precise representation than the abstract one.

Taken together, these results not only provide evidence that EVC is recruited during haptic exploration of objects, but also demonstrate that stimulus dimensions can be discriminated based on activity patterns in the visual cortex despite the lack of visual input, and that this information cannot be merely attributed to visual imagery. Our findings also give an overview of the brain networks supporting the representation of stimulus size both within and across Haptic exploration and Visual imagery. Specifically, while haptically explored size can be decoded in early visual areas, higher-order parietal and premotor regions encode size information across the two tasks. This suggests that these regions may play a pivotal role in abstracting perceptual representations independently of the task modality. In line with this view, IPS has been associated with the processing of object-related features (Konen and Kastner, 2008; Mruczek et al., 2013; for a review, see Erlikhman et al., 2018) and with multisensory processing mechanisms (Huang and Sereno, 2018). Additionally, dPM area has been found to process both intrinsic and extrinsic object properties (e.g., size and location), which are relevant for accurately positioning our digits during grasping actions (Monaco et al., 2015).

4.1. Occipital and temporal areas

So far, several neuroimaging studies have investigated the role of visual areas in haptic object exploration without visual input. However, most of these studies have used a univariate approach, which reveals whether an area is engaged during haptic exploration but does not provide information about the content-specific nature of the elicited activity patterns. Moreover, the majority of these previous studies has focused on haptic shape (Monaco et al., 2017; Snow et al., 2014), texture (Eck et al., 2013; Sathian et al., 2011; Stilla and Sathian, 2008), and dot patterns processing (Merabet et al., 2007), leaving the neural mechanisms underlying haptic size processing relatively underexplored. Yet, object size is critical, as it is an inherently relevant object property that guides hand actions.

Evidence from several neuroimaging studies supports the involvement of visual cortical areas in haptic shape processing, including the lateral occipital complex (LOC) in the ventral visual stream and EVC (Lee Masson et al., 2016; Monaco et al., 2017; Snow et al., 2014). Further, the occipital cortex has a modality-independent representation (i.e., shared across haptic and vision) of basic shape features like curvature and rectilinearity (Tian et al., 2023). Interestingly, haptic exploration of object shape in the dark also activates the foveal representation in the OP (Monaco et al., 2017). This suggests that tactile information about the shape of objects can recruit high-acuity visual processing areas, even when objects are explored in the absence of visual input. Our results extend these findings by showing that LOtv, V1, and OP are engaged during haptic exploration of stimuli in blindfolded participants, and that haptic size information is represented in these areas. The representation of haptic size in LOtv is in line with the known foveal representation in this region and may reflect cross-talk between the broader lateral occipital complex and the OP. Despite evidence of haptic information content being represented in early and higher-order visual areas, their causal role in haptic perception remains unclear. Causal evidence from a patient with bilateral LOC lesions has challenged the notion that the ventral visual stream plays a critical role in haptic object recognition. Notably, despite the absence of LOC activation, the patient exhibited intact haptic shape recognition and preserved activation in regions of the dorsal visual stream (Snow et al., 2015). This dissociation suggests that, although LOC is fundamental for visual size processing in neurologically intact individuals and is engaged even earlier than the EVC (Zeng et al., 2020), LOtv, a subregion of LOC, is recruited during haptic tasks but may not be essential for haptic recognition. We found haptic size representation also in ITS, a ventral visual stream area involved in object recognition. This result is in agreement with a previous univariate fMRI study (Merabet et al., 2007), which showed that tactile exploration of raised-dot patterns recruited brain regions including V1 and, to a lesser extent, a region in the ventral occipital and inferior temporal cortex (ITC). Overall, these findings support the idea that both early and higher-order visual cortical areas contribute to haptic information processing, regardless of the specific task (i.e., haptic exploration of size, shapes, or dot patterns).

Although a recent study has investigated the brain regions involved in representing haptic size information (Perini et al., 2020), a direct comparison between haptic exploration and visual imagery of differently sized stimuli, especially in early visual areas, has not yet been examined. More specifically, Perini et al. (2020) examined the brain regions involved in haptic judgements of object size by applying searchlight MVPA to fMRI data. The authors found that areas of the IPS and the lateral prefrontal cortex contain a representation of haptic size that is independent of the hand used (either left or right). However, they did not find such representations in occipital and temporal areas. As the authors pointed out, one possible explanation is that the occipital and temporal lobes were not fully covered during fMRI data acquisition in some participants. As such, the lack of data from these areas makes it difficult to draw conclusions on the role of ventral visual stream areas in encoding haptic size information from their study. Additional methodological differences could also account for the discrepancy in results compared to our study. For example, while Perini et al. (2020) asked participants to perform a haptic size comparison task using either hand with a movement similar to a pincer grasp, in our experiment participants explored three differently sized rings using the thumb and index finger of their dominant right hand. These methodological differences may have contributed to the detection of haptic size information in the occipital and temporal cortices.

One possible explanation for the involvement of visual areas in haptic object perception is that their recruitment is mediated by top-down visual imagery processes and, therefore, may not be essential for haptic processing.

In line with this hypothesis, an fMRI study by Lee Masson et al. (2016) showed that haptic shape representations could be detected in the EVC and the right LOC, but only when participants had prior visual experience with the objects. Based on this evidence, the authors proposed that top-down mechanisms may engage visual imagery to support haptic shape processing. As for the role of EVC in visual imagery and perception, a recent fMRI study using voxel-wise encoding models, revealed that neural representations in early visual areas (like V1) during imagery resemble those activated during actual visual perception, not only for simple, Gabor-like features (i.e., oriented edge-detection features), but also for more complex ones (Huang et al., 2023). This supports the idea that imagery and perception share overlapping neural substrates in the EVC. However, while this may be true for visual perception, the same might not apply to haptic perception in the EVC. Furthermore, although it may be tempting to attribute the significant Haptic size decoding in early visual areas to visual imagery, our results show that visually imagined size cannot be accurately decoded in either V1 or OP. Besides, we found a significant difference between the accuracy of Haptic and Visual imagery size decoding in left

OP and right V1. It is important to note that the absence of Visually imagery size decoding in early visual areas may reflect the fact that participants never had visual experience of the stimulus, neither before nor during the experiment. It might also be argued that the lack of significant visually imagined size discrimination based on activity patterns in these areas is likely due to a lower signal-to-noise ratio in the Visual imagery than Haptic task. Another possible interpretation of the results in the EVC is that the Haptic exploration task does involve visual imagery to some extent, as imagery may be facilitated by the tactile referent making Haptic size decoding more robust and significant. Along the same lines, the lack of tactile input during the pure Visual imagery task might hamper decoding of visually imagined size. However, if this were the case, we would expect Visual imagery size decoding to be similarly unreliable across all ROIs. Instead, we found significant decoding of visually imagined size in ventral and dorsal stream regions such as the left LOtv, SMA, bilateral dPM, and IPS, indicating that the imagery signal was robust enough to yield significant decoding in brain regions that are known to be involved in imagery representations. In addition, if tactile information was sufficient to boost visual imagery during the Haptic task, then significant cross-decoding should occur whenever both Haptic and Visual imagery size decoding are significant as the visual imagery component should be present in both conditions. Yet, the fact that both left SMA and left LOtv showed successful decoding of visually imagined and haptically explored size, but not across tasks makes it unlikely that the tasks share similar representational content represented by visual imagery.

We found no significant correlation between VVIQ and Visual imagery size decoding in the EVC. This result is in line with previous findings showing a lack of correlation, in the EVC, between VVIQ and pure visual imagery decoding of common objects varying in orientation, shape, and colour (e.g., car, lamp, umbrella, etc.), although a significant correlation was found between VVIQ and the decoding across visual imagery and visual perception (Lee et al., 2012). The lack of correlation in EVC supports the idea that activity patterns might not reflect the subjective offline evaluations regarding the vividness and strength of visual imagery. One possible explanation for the lack of correlation is associated with the different nature of the visual imagery content assessed with VVIQ and the one required by our Visual imagery task. While our stimuli might be so basic that participants did not have to summon effortful visual imagery to mentally visualize them, the VVIQ assesses the ability to vividly visually imagine more complex scenes and objects. Therefore, the vividness of one's visual imagery as assessed by the VVIQ might not correlate with the decoding accuracies of imagined size of basic stimuli. However, we found a significant correlation between VVIQ scores and Visual imagery size decoding accuracies in left preSMA which provides evidence against this interpretation. Another possibility is that the lack of correlation might be due to the fact that participants were never allowed to view the stimuli. With no prior visual experience, it may have been difficult for them to generate visual mental images of the rings, even if we instructed them to engage in visual imagery. Nevertheless, the haptic size representation observed in early visual cortical areas in our study cannot be explained entirely by visual imagery.

Interestingly we found that the left LOtv stores a flexible representation of object size that is independent of whether participants were imagining or haptically exploring the stimuli. This finding indicates that the left LOtv encodes size-based spatial information in a format that is not strictly bound to one task modality, but rather, is available as a size-related magnitude representation accessible across tasks. Notably, such size-sensitive regions may share a common functional architecture with temporal lobe networks that specialize in the processing of allocentric, object-centered spatial information. For example, Schenk (2006) showed that patient D.F., who suffers from bilateral ventral stream lesions, exhibits an allocentric rather than a purely perceptual deficit, implying that object-based spatial metrics (e.g., relative position and size in space) processed in the ventral visual stream are crucial for certain types of visuomotor tasks. Likewise, the frameworks proposed by Goodale and Haffenden (1998) and further elaborated in Milner and Goodale's reviews (2006, 2008) emphasize that distinct neural streams, including those in the temporal lobe, preferentially process spatial metrics that afford object-centered (allocentric) reference frames. Taken as a whole, these findings reinforce the idea that the left LOtv may be part of a broader network of size-sensitive regions that encode spatial information in an object-based (allocentric) manner, that is accessible across both imagery and haptic modalities.

While there is evidence showing that LOtv is a multimodal area processing both visual and tactile information (Lacey et al., 2009), there is no clear evidence for its involvement in imagery processes. Previous work has shown that the lateral occipital complex (LOC), which contains LOtv, is involved in imagery of haptically explored shapes (Lee Masson et al., 2016; Zhang et al., 2004). In a recent review, Spagna et al. (2024) have proposed a heterarchical neural architecture at the basis of visual imagery which involves both domain-general and domain-specific neural mechanisms. The authors identified a region in the left mid-fusiform gyrus, along with frontoparietal areas, as core components of the network supporting visual imagery regardless of the semantic domain (e.g., faces, colours, shapes imagery). Moreover, the authors provided evidence that imagery and visual perception recruit similar cortical regions both in the ventral and dorsal visual streams if the content is from a preferred domain (e.g., fusiform face areas for faces and parahippocampal place area for places; O'Craven and Kanwisher, 2000). While Spagna et al. (2024) highlighted the shared engagement of domain-preferring regions during visual perception and imagery, our findings extend this framework by showing that a shape selective region in the ventral stream, such as LOtv, supports both visual imagery and haptic perception through distinct neural mechanisms.

Why would the EVC and ventral stream areas, known to primarily process visual information, code the size of haptically explored stimuli? It is possible that the visual system predicts and simulates the expected size of a haptically explored object based on prior experience, in order to assess whether the haptic input matches the internal visual prediction and, if not, update the internal model accordingly.

Predicting an object's visual size from haptics is computationally efficient, and since we often use vision to confirm what we touch, the visual system may be deeply embedded in this prediction loop. In our daily life, we often see what we touch, leading to frequent co-activation of visual and somatosensory cortices. As such, it is possible that signals from one sensory modality trigger activation also in other sensory areas. Hence, the recruitment of EVC for non-visual, haptic tasks is likely due to feedback signals coming from sensory-motor brain regions, as indicated by the results of the PPI analysis.

The occipitotemporal cortex contains neural representations of the real-world size of visually presented objects (Coutanche and Koch, 2018), suggesting that semantic information might also play a role. To minimize potential semantic processing related to ring size we used letter-based instructions which were randomly assigned to size conditions across participants. Moreover, semantic information is typically linked to object identity, whereas in our study the stimuli were simple geometric shapes (i.e., rings) with the same identity. If our rings had been associated with real-world objects of corresponding sizes, thereby engaging semantic size processing during both the Haptic exploration and Visual imagery tasks, we would expect significant decoding of size in the Visual imagery condition and possibly also in the Cross-decoding condition, particularly in early visual areas but not in more anterior temporal regions, in line with the study by Coutanche and Koch (2018). This pattern contrasts with our findings, making a semantic explanation unlikely.

4.2. Frontal and parietal areas

Our Haptic exploration task required the active movement of the thumb and index finger to extract size-related features. These

movements inherently demand the dynamic coordination of finger aperture and trajectories, which varied slightly across our differently sized stimuli. The acquired sensory inputs are integrated within the haptic system, known to be subserved by a network of frontal and parietal regions (James et al., 2007; Sathian, 2016). Consistent with this notion, we observed successful decoding of stimulus size based on Haptic trials across all frontal and parietal ROIs. Specifically, Haptic size decoding in M1/S1 likely reflects a combination of afferent cutaneous and proprioceptive input, as well as kinematic differences related to the motor execution of exploration strategies for the three different sizes, such as adjustments in grip aperture and spatial scaling of finger movements. Interestingly, right M1/S1 showed a significant negative correlation between vividness imagery scores and Haptic size decoding accuracy. This result suggests that participants with higher vividness of visual imagery, compared to those with low imagery vividness, have a haptic size representation that is likely less dependent on motor and somatosensory information. Instead, participants who score low on VVIQ might rely more on haptic and kinesthetic information to represent size information when haptically exploring it.

Beyond M1/S1, successful decoding of haptic stimulus size was also observed in a distributed frontoparietal network, notably including bilateral dPM and vPM, aIPS and pIPS, SMA, and preSMA. This pattern partially aligns with previous findings showing that these regions, especially aIPS, dPM and SMA, are involved in processing intrinsic object properties, such as size, and integrating them with action-relevant spatial information during grasping (e.g., Monaco et al., 2015), making them key regions for sensorimotor transformations. Specifically, decoding in aIPS and pIPS is especially informative. Here, we observed successful decoding of size not only in Haptic but also Visual imagery trials, and across the two tasks. The IPS is well-known for its role in sensorimotor integration as well as in visual imagery (Spagna et al., 2021). Interestingly, both regions have also been implicated in supramodal encoding of spatial and metric object features (Reed et al., 2005; Stilla and Sathian, 2008), suggesting a high-level representation of properties such as size that transcends input modality. Furthermore, Harvey et al. (2015) found that the human parietal cortex contains topographic maps for visually processed object size, similar to those for numerosity. These maps overlap, though not completely, suggesting a spatial organization that is shared across different types of quantity information. This further supports the role of the IPS in abstract processing of size information. Therefore, the engagement of the IPS during both haptically explored and visually imagined size conditions, and across conditions, is consistent with its role as a hub where multimodal spatial information converge into a unified representation that is also accessed during visual imagery. The successful decoding of size in the dorsal visual stream aligns well with neuropsychological data from patients with ventral visual stream lesions. In particular, patients with severe visual agnosia resulting from bilateral ventral pathway damage showed spared recognition of graspable objects, but only when their physical size matched the expected real-world size (Holler et al., 2019). Although this study did not investigate haptic perception, their finding is in line with our results showing more widespread size decoding in dorsal than ventral visual stream areas, as the dorsal visual stream links visual and real-world action-related object information.

The dPM also showed robust decoding not only within both Haptic and Visual imagery trials, but also across the two tasks. Although dPM is not consistently engaged during visual imagery across studies (Spagna et al., 2021), it is possible that when participants imagine the size of circles, an interaction between visual and somatosensory representations occurs to create a spatial or metric map in the brain. This process could involve regions like the IPS and possibly the dPM, depending on the task context. The observed size decoding across Haptic exploration and Visual imagery tasks in dPM aligns with the multimodal functions attributed to the premotor cortex (Hardwick et al., 2018).

The size of a stimulus is indicative of whether and how an object can be grasped and manipulated, and helps predict its weight. This information is essential for planning accurate grasping movements. As such, the abstract representation of size is unsurprising in areas that are well-known to be involved in grasping actions, such as aIPS, pIPS, and dPM (for reviews, see Culham et al., 2006; Gallivan and Culham, 2015). These findings reinforce the idea that the degree of content-similarity (stimulus size) across tasks (Haptic exploration and Visual imagery) is strongly dependent on the degree of specialization of a brain area in processing that particular content for action, such as the aIPS, pIPS, and dPM for grasping movements.

Interestingly, the left SMA showed decoding of haptically explored but also imagined size, although no cross-modal size decoding was found here. This pattern of results was also observed in left LOtv, suggesting that both regions represent size-related magnitude information in a context-dependent way. Our results align with previous research showing that the left SMA is involved in visual imagery (for a meta-analysis, see Spagna et al., 2021). In addition, they also reveal that the higher the Visual imagery size decoding accuracy in the left preSMA, the greater the visual imagery vividness. These findings are consistent with the prominent role of frontoparietal areas in sustaining imagery over time, as this process relies on working memory mechanisms supported by the same frontoparietal, especially prefrontal, networks (Miller et al., 2018). The preSMA is strongly involved in motor imagery (for a meta-analysis, see Hardwick et al., 2018) and the SMA proper exerts a strong inhibitory effect on the forward connection to M1 during motor imagery (Kasess et al., 2008). This mechanism is likely responsible for preventing the execution of internally simulated actions and might also involve the preSMA along with the SMA proper.

4.3. PPIs: functional connectivity during the Haptic task

The representation of size information in the EVC is likely due to the stronger functional connections during the Haptic exploration than Visual imagery task with areas involved in multimodal perception, like the LOtv (Amedi et al., 2001), and haptic shape processing of objects for subsequent actions, like the aIPS (Króliczak et al., 2008; Marangon et al., 2016; Monaco et al., 2017). The functional connection between the EVC and ventral and dorsal stream areas has already been found during haptic shape exploration in the dark (Monaco et al., 2017). Here, we confirm and extend those findings by showing that haptic size processing is also supported by functional connections between the EVC and ventral as well as dorsal visual stream areas, and premotor cortex.

4.4. Limitations

One limitation of the current study is related to the possible recruitment of mental motor imagery during our Visual imagery task. Although we specifically asked our participants to visually imagine the size of the stimulus they had previously explored, we cannot completely rule out the possibility that participants, even involuntarily, also visually imagined the exploratory movement associated with a given size. In fact, while they did not have any prior visual experience of the stimulus, they could still rely on previous haptic experience with the same stimulus, which, in turn, could have helped them create a visual mental image of the associated size during the Visual imagery task. Additionally, participants may have engaged in tactile imagery as the major source of information about the stimulus was the haptic system, as discussed in Sections 2.2. and 4.1.

5. Conclusions

By applying MVPA to fMRI data, we demonstrated for the first time that information about stimulus size can be decoded not only during haptic exploration but also during visual imagery of unseen stimuli. First, we found that early visual areas, including V1 and OP, successfully decoded haptic but not visually imagined size, suggesting that haptic processing in the EVC does not simply reflect visual imagery of the

haptically explored stimulus. Instead, higher-order and associative regions, such as LOtv, aIPS, pIPS, dPM, and SMA, showed overlapping but distinct representations of size for both Haptic and Visual imagery tasks. Second, cross-decoding yielded significant results in parietal and premotor areas, including dPM, aIPS, and pIPS, thus suggesting the existence of an abstract representation of size that is independent of the task demands. Overall, these findings advance our understanding of how the brain represents object properties when we haptically explore and visually imagine them. While the EVC represents haptic size information, associative areas show overlapping but distinct representations of haptic and visually imagined size, respectively. Last, but not less important, the premotor and parietal cortices have a shared representation of size.

Funding

This work was supported by the European Commission and the Italian Ministry of University and Research within the Next generation EU programme Young Researchers [grant number 40104258]. Project title: "PrefAcE, Predictions for Action Execution: the neural basis of movement intention".

Declaration of generative AI and AI-assisted technologies in the writing process

During the preparation of this work the Authors used ChatGPT in order to improve the readability of the manuscript. After using this tool, the Authors reviewed and edited the content as needed and take full responsibility for the content of the published article.

Data availability

The data that support the findings of this study are available from the corresponding author, S.M., and the first author, S.S., upon request.

CRediT authorship contribution statement

Samantha Sartin: Writing – original draft, Visualization, Resources, Project administration, Methodology, Investigation, Formal analysis, Data curation. **Federica Danaj:** Writing – review & editing, Resources, Methodology, Investigation, Formal analysis, Data curation. **Fabio Del Giudice:** Writing – review & editing, Resources, Investigation. **Juan Chen:** Writing – review & editing, Methodology, Conceptualization. **Dietrich Samuel Schwarzkopf:** Writing – review & editing, Methodology, Conceptualization. **Irene Sperandio:** Writing – review & editing, Methodology, Conceptualization. **Simona Monaco:** Writing – review & editing, Validation, Supervision, Resources, Project administration, Methodology, Funding acquisition, Conceptualization.

Declaration of competing interest

The authors declare that they have no known competing financial interests or personal relationships that could have appeared to influence the work reported in this paper.

Acknowledgements

We thank all participants for their time and feedback on the experiment, Lorenzo Moschini for help with the 3D printer, and Federica Anzini for help with cortex segmentation.

Supplementary materials

Supplementary material associated with this article can be found, in the online version, at doi:10.1016/j.neuroimage.2026.121774.

References

Amedi, A., Malach, R., Hendler, T., Peled, S., Zohary, E., 2001. Visuo-haptic object-related activation in the ventral visual pathway. Nat. Neurosci. 4 (3), 324–330. https://doi.org/10.1038/85201.

Benjamini, Y., Hochberg, Y., 1995. Controlling the false discovery rate: a practical and powerful approach to multiple testing. J. R. Stat. Soc. B: Stat. Methodol. 57 (1), 289–300. https://doi.org/10.1111/j.2517-6161.1995.tb02031.x.

Bracci, S., Op de Beeck, H.P., 2023. Understanding Human object vision: a picture is worth a thousand representations. Annu. Rev. Psychol. 74, 113–135. https://doi.org/10.1146/ANNUREV-PSYCH-032720-041031.

Cavina-Pratesi, C., Goodale, M.A., Culham, J.C., 2007. FMRI reveals a dissociation between grasping and perceiving the size of real 3D objects. PLOS ONE 2 (5), e424. https://doi.org/10.1371/JOURNAL.PONE.0000424.

Coutanche, M.N., Koch, G.E., 2018. Creatures great and small: real-world size of animals predicts visual cortex representations beyond taxonomic category. NeuroImage 183, 627–634. https://doi.org/10.1016/j.neuroimage.2018.08.066.

Cui, X., Jeter, C.B., Yang, D., Montague, P.R., Eagleman, D.M., 2007. Vividness of mental imagery: individual variability can be measured objectively. Vis. Res. 47 (4), 474–478. https://doi.org/10.1016/j.visres.2006.11.013.

Culham, J.C., Cavina-Pratesi, C., Singhal, A., 2006. The role of parietal cortex in visuomotor control: what have we learned from neuroimaging? Neuropsychologia 44 (13), 2668–2684. https://doi.org/10.1016/J.NEUROPSYCHOLOGIA.2005.11.003.

Culham, J.C., Danckert, S.L., DeSouza, J.F.X., Gati, J.S., Menon, R.S., Goodale, M.A., 2003. Visually guided grasping produces fMRI activation in dorsal but not ventral stream brain areas. Exp. Brain Res. 153 (2), 180–189. https://doi.org/10.1007/s00221-003-1591-5.

Eck, J., Kaas, A.L., Goebel, R., 2013. Crossmodal interactions of haptic and visual texture information in early sensory cortex. NeuroImage 75, 123–135. https://doi.org/10.1016/J.NEUROIMAGE.2013.02.075.

Erlikhman, G., Caplovitz, G.P., Gurariy, G., Medina, J., Snow, J.C., 2018. Towards a unified perspective of object shape and motion processing in human dorsal cortex. Conscious. Cogn. 64, 106–120. https://doi.org/10.1016/J.CONCOG.2018.04.016.

Filimon, F., 2010. Human cortical control of hand movements: parietofrontal networks for reaching, grasping, and pointing. Neuroscientist 16 (4), 388–407. https://doi.org/10.1177/1073858410375468.

Forman, S.D., Cohen, J.D., Fitzgerald, M., Eddy, W.F., Mintun, M.A., Noll, D.C., 1995. Improved assessment of significant activation in Functional Magnetic Resonance Imaging (fMRI): use of a cluster-size threshold. Magn. Reson. Med. 33 (5), 636–647. https://doi.org/10.1002/mrm.1910330508.

Friston, K.J., Buechel, C., Fink, G.R., Morris, J., Rolls, E., Dolan, R.J., 1997. Psychophysiological and modulatory interactions in neuroimaging. NeuroImage 6 (3), 218–229. https://doi.org/10.1006/nimg.1997.0291.

Friston, K.J., Holmes, A.P., Price, C.J., Büchel, C., Worsley, K.J., 1999. Multisubject fMRI studies and conjunction analyses. NeuroImage 10 (4), 385–396. https://doi.org/10.1006/nimg.1999.0484.

Gallivan, J.P., Culham, J.C., 2015. Neural coding within human brain areas involved in actions. Curr. Opin. Neurobiol. 33, 141–149. https://doi.org/10.1016/J.CONB.2015.03.012.

Gallivan, J.P., McLean, D.A., Valyear, K.F., Pettypiece, C.E., Culham, J.C., 2011. Decoding action intentions from preparatory brain activity in human parieto-frontal networks. J. Neurosci. 31 (26), 9599–9610. https://doi.org/10.1523/JNEUROSCI.0080-11.2011.

Goebel, R., Esposito, F., Formisano, E., 2006. Analysis of Functional Image Analysis Contest (FIAC) data with BrainVoyager QX: from single-subject to cortically aligned group General Linear Model analysis and self-organizing group Independent Component Analysis. Hum. Brain Mapp. 27 (5), 392–401. https://doi.org/10.1002/hbm.20249.

Goodale, M.A., Haffenden, A., 1998. Frames of reference for perception and action in the Human visual system. Neurosci. Biobehav. Rev. 22 (2), 161–172. https://doi.org/10.1016/S0149-7634(97)00007-9.

Hardwick, R.M., Caspers, S., Eickhoff, S.B., Swinnen, S.P., 2018. Neural correlates of action: comparing meta-analyses of imagery, observation, and execution. Neurosci. Biobehav. Rev. 94, 31–44. https://doi.org/10.1016/J.NEUBIOREV.2018.08.003.

Harvey, B.M., Fracasso, A., Petridou, N., Dumoulin, S.O., 2015. Topographic representations of object size and relationships with numerosity reveal generalized quantity processing in human parietal cortex. Proc. Natl. Acad. Sci. U. S. A. 112 (44), 13525–13530. https://doi.org/10.1073/PNAS.1515414112.

Holler, D.E., Behrmann, M., Snow, J.C., 2019. Real-world size coding of solid objects, but not 2-D or 3-D images, in visual agnosia patients with bilateral ventral lesions. Cortex 119, 555–568. https://doi.org/10.1016/j.cortex.2019.02.030.

Huang, R.S., Sereno, M.I., 2018. Multisensory and sensorimotor maps. In: Vallar, Giuseppe, Branch Coslett, H. (Eds.), Handbook of Clinical Neurology, Handbook of Clinical Neurology, 151. Elsevier, pp. 141–161. https://doi.org/10.1016/B978-0-444-63622-5.00007-3.

Huang, Y., Pollick, F., Liu, M., Zhang, D., 2023. Gabor and Non-Gabor Neural Representations are shared between visual perception and mental imagery. J. Cogn. Neurosci. 35 (6), 1045–1060. https://doi.org/10.1162/JOCN_A_01992.

James, T.W., Kim, S., Fisher, J.S., 2007. The neural basis of haptic object processing. Can. J. Exp. Psychol. 61 (3), 219–229. https://doi.org/10.1037/cjep2007023.

Kasess, C.H., Windischberger, C., Cunnington, R., Lanzenberger, R., Pezawas, L., Moser, E., 2008. The suppressive influence of SMA on M1 in motor imagery revealed by fMRI and dynamic causal modeling. NeuroImage 40 (2), 828–837. https://doi.org/10.1016/J.NEUROIMAGE.2007.11.040.

Konen, C.S., Kastner, S., 2008. Two hierarchically organized neural systems for object information in human visual cortex. Nat. Neurosci. 11 (2), 224–231. https://doi.org/10.1038/NN2036.

Kriegeskorte, N., Bandettini, P., 2007. Combining the tools: activation- and information-based fMRI analysis. NeuroImage 38 (4), 666–668. https://doi.org/10.1016/j.neuroimage.2007.06.030.

Kriegeskorte, N., Lindquist, M.A., Nichols, T.E., Poldrack, R.A., Vul, E., 2010. Everything you never wanted to know about circular analysis, but were afraid to ask. J. Cereb. Blood Flow Metab. 30, 1551–1557. https://doi.org/10.1038/jcbfm.2010.86.

Króliczak, G., McAdam, T.D., Quinlan, D.J., Culham, J.C., 2008. The human dorsal stream adapts to real actions and 3D shape processing: a functional magnetic resonance imaging study. J. Neurophysiol. 100 (5), 2627–2639. https://doi.org/10.1152/jn.01376.2007.

Lacey, S., Sathian, K., 2014. Visuo-haptic multisensory object recognition, categorization, and representation. Front. Psychol. 5, 730. https://doi.org/10.3389/FPSYG.2014.00730.

Lacey, S., Tal, N., Amedi, A., Sathian, K., 2009. A putative model of multisensory object representation. Brain Topogr. 21 (3–4), 269–274. https://doi.org/10.1007/S10548-009-0087-4.

Lee Masson, H., Bulthé, J., Op de Beeck, H.P., Wallraven, C., 2016. Visual and haptic shape processing in the Human brain: unisensory processing, multisensory convergence, and top-down influences. Cereb. Cortex 26 (8), 3402–3412. https://doi.org/10.1093/CERCOR/BHV170.

Lee, S.H., Kravitz, D.J., Baker, C.I., 2012. Disentangling visual imagery and perception of real-world objects. NeuroImage 59 (4), 4064–4073. https://doi.org/10.1016/J.NEUROIMAGE.2011.10.055.

Marangon, M., Kubiak, A., Króliczak, G., 2016. Haptically guided grasping. fMRI shows right-hemisphere parietal stimulus encoding, and bilateral dorso-ventral parietal gradients of object-and action-related processing during grasp execution. Front. Hum. Neurosci. 9, 691. https://doi.org/10.3389/fnhum.2015.00691.

Marks, D.F., 1995. New directions for mental imagery research. J. Ment. Imag. 19 (3–4), 153–167.

McLaren, D.G., Ries, M.L., Xu, G., Johnson, S.C., 2012. A generalized form of context-dependent psychophysiological interactions (gPPI): a comparison to standard approaches. NeuroImage 61 (4), 1277–1286. https://doi.org/10.1016/j.neuroimage.2012.03.068.

Merabet, L.B., Swisher, J.D., Mcmains, S.A., Halko, M.A., Amedi, A., Pascual-Leone, A., Somers, D.C., 2007. Combined activation and deactivation of visual cortex during tactile sensory processing. J. Neurophysiol. 97 (2), 1633–1641. https://doi.org/10.1152/jn.00806.2006.

Miller, E.K., Lundqvist, M., Bastos, A.M., 2018. Working memory 2.0. Neuron 100 (2), 463–475. https://doi.org/10.1016/J.NEURON.2018.09.023.

Milner, A.D., Goodale, M.A., 2006. The Visual Brain in Action, 2nd ed. Oxford University Press. https://doi.org/10.1093/acprof:oso/9780198524724.001.0001.

Milner, A.D., Goodale, M.A., 2008. Two visual systems re-viewed. Neuropsychologia 46 (3), 774–785. https://doi.org/10.1016/J.NEUROPSYCHOLOGIA.2007.10.005.

Monaco, S., Chen, Y., Medendorp, W.P., Crawford, J.D., Fiehler, K., Henriques, D.Y.P., 2014. Functional magnetic resonance imaging adaptation reveals the cortical networks for processing grasp-relevant object properties. Cereb. Cortex 24 (6), 1540–1554. https://doi.org/10.1093/cercor/bht006.

Monaco, S., Gallivan, J.P., Figley, T.D., Singhal, A., Culham, J.C., 2017. Recruitment of foveal retinotopic cortex during haptic exploration of shapes and actions in the dark. J. Neurosci. 37 (48), 11572–11591. https://doi.org/10.1523/JNEUROSCI.2428-16.2017.

Monaco, S., Malfatti, G., Zendron, A., Pellencin, E., Turella, L., 2019. Predictive coding of action intentions in dorsal and ventral visual stream is based on visual anticipations, memory-based information and motor preparation. Brain Struct. Funct. 224 (9), 3291–3308. https://doi.org/10.1007/s00429-019-01970-1.

Monaco, S., Sedda, A., Cavina-Pratesi, C., Culham, J.C., 2015. Neural correlates of object size and object location during grasping actions. Eur. J. Neurosci. 41 (4), 454–465. https://doi.org/10.1111/EJN.12786.

Moretto, G., di Pellegrino, G., 2008. Grasping numbers. Exp. Brain Res. 188, 505–515. https://doi.org/10.1007/s00221-008-1386-9.

Mruczek, R.E.B., von Loga, I.S., Kastner, S., 2013. The representation of tool and non-tool object information in the human intraparietal sulcus. J. Neurophysiol. 109 (12), 2883–2896. https://doi.org/10.1152/JN.00658.2012.

O'Craven, K.M., Kanwisher, N., 2000. Mental imagery of faces and places activates corresponding stimulus-specific brain regions. J. Cogn. Neurosci. 12 (6), 1013–1023. https://doi.org/10.1162/08989290051137549.

Ogawa, S., Tank, D.W., Menon, R., Ellermann, J.M., Kim, S.G., Merkle, H., Ugurbil, K., 1992. Intrinsic signal changes accompanying sensory stimulation: functional brain mapping with magnetic resonance imaging. Proc. Natl. Acad. Sci. U. S. A. 89 (13), 5951–5955. https://doi.org/10.1073/pnas.89.13.5951.

Oosterhof, N.N., Connolly, A.C., Haxby, J.V., 2016. CoSMoMVPA: multi-modal multivariate pattern analysis of neuroimaging data in Matlab/GNU Octave. Front. Neuroinformatics 10, 27. https://doi.org/10.3389/fninf.2016.00027.

Oosterhof, N.N., Wiestler, T., Downing, P.E., Diedrichsen, J., 2011. A comparison of volume-based and surface-based multi-voxel pattern analysis. NeuroImage 56 (2), 593–600. https://doi.org/10.1016/j.neuroimage.2010.04.270.

O'Reilly, J.X., Woolrich, M.W., Behrens, T.E., Smith, S.M., Johansen-Berg, H., 2012. Tools of the trade: psychophysiological interactions and functional connectivity. Soc. Cogn. Affect. Neurosci. 7 (5), 604–609. https://doi.org/10.1093/scan/nss055.

Perini, F., Powell, T., Watt, S.J., Downing, P.E., 2020. Neural representations of haptic object size in the human brain revealed by multivoxel fMRI patterns. J. Neurophysiol. 124 (1), 218–231. https://doi.org/10.1152/JN.00160.2020.

Reed, C.L., Klatzky, R.L., Halgren, E., 2005. What vs. where in touch: an fMRI study. NeuroImage 25 (3), 718–726. https://doi.org/10.1016/J.NEUROIMAGE.2004.11.044.

Sadato, N., Pascual-Leone, A., Grafman, J., Deiber, M.P., Ibañez, V., Hallett, M., 1998. Neural networks for Braille reading by the blind. Brain 121 (7), 1213–1229. https://doi.org/10.1093/BRAIN/121.7.1213.

Sathian, K., 2016. Analysis of haptic information in the cerebral cortex. J. Neurophysiol. 116 (4), 1795–1806. https://doi.org/10.1152/jn.00546.2015.

Sathian, K., Lacey, S., Stilla, R., Gibson, G.O., Deshpande, G., Hu, X., LaConte, S., Glielmi, C., 2011. Dual pathways for haptic and visual perception of spatial and texture information. NeuroImage 57 (2), 462–475. https://doi.org/10.1016/J.NEUROIMAGE.2011.05.001.

Schenk, T., 2006. An allocentric rather than perceptual deficit in patient D.F. Nat. Neurosci. 9 (11), 1369–1370. https://doi.org/10.1038/nn1784. *2006 9:11*.

Silva, P.R., Farias, T., Cascio, F., Dos Santos, L., Peixoto, V., Crespo, E., Ayres, C., Ayres, M., Marinho, V., Bastos, V.H., Ribeiro, P., Velasques, B., Orsini, M., Fiorelli, R., de Freitas, M.R.G., Teixeira, S., 2018. Neuroplasticity in visual impairments. Neurol. Int. 10 (4), 7326. https://doi.org/10.4081/ni.2018.7326.

Singhal, A., Monaco, S., Kaufman, L.D., Culham, J.C., 2013. Human fMRI reveals that delayed action re-recruits visual perception. PLoS One 8 (9), e73629. https://doi.org/10.1371/JOURNAL.PONE.0073629.

Snow, J.C., Goodale, M.A., Culham, J.C., 2015. Preserved haptic shape processing after bilateral LOC lesions. J. Neurosci. 35 (40), 13745–13760. https://doi.org/10.1523/JNEUROSCI.0859-14.2015.

Snow, J.C., Strother, L., Humphreys, G.W., 2014. Haptic shape processing in Visual cortex. J. Cogn. Neurosci. 26 (5), 1154–1167. https://doi.org/10.1162/jocn_a_00548.

Spagna, A., Hajhajate, D., Liu, J., Bartolomeo, P., 2021. Visual mental imagery engages the left fusiform gyrus, but not the early visual cortex: a meta-analysis of neuroimaging evidence. Neurosci. Biobehav. Rev. 122, 201–217. https://doi.org/10.1016/j.neubiorev.2020.12.029.

Spagna, A., Heidenry, Z., Miselevich, M., Lambert, C., Eisenstadt, B.E., Tremblay, L., Liu, Z., Liu, J., Bartolomeo, P., 2024. Visual mental imagery: evidence for a heterarchical neural architecture. Phys. Life Rev. 48, 113–131. https://doi.org/10.1016/J.PLREV.2023.12.012.

Stilla, R., Sathian, K., 2008. Selective visuo-haptic processing of shape and texture. Hum. Brain Mapp. 29 (10), 1123–1138. https://doi.org/10.1002/HBM.20456.

Talairach, J., Tournoux, P., 1988. Co-planar stereotaxic atlas of the human brain-3-dimensional proportional system. Approach Cereb. Imaging.

Tian, S., Chen, Y., Fu, Z., Wang, X., Bi, Y., 2023. Simple shape feature computation across modalities: convergence and divergence between the ventral and dorsal visual streams. Cereb. Cortex 33 (15), 9280–9290. https://doi.org/10.1093/CERCOR/BHAD200.

Vul, E., Kanwisher, N., 2010. Begging the question: the non-independence error in fMRI data analysis. In: Hanson, S.J., Bunzl, M. (Eds.), Foundational Issues in Human Brain Mapping. The MIT Press, pp. 71–91. doi:10.7551/mitpress/9780262014021.003.0007.

Zeng, H., Fink, G.R., Weidner, R., 2020. Visual size processing in early Visual cortex follows lateral occipital cortex involvement. J. Neurosci. 40 (22), 4410–4417. https://doi.org/10.1523/JNEUROSCI.2437-19.2020.

Zhang, M., Weisser, V.D., Stilla, R., Prather, S.C., Sathian, K., 2004. Multisensory cortical processing of object shape and its relation to mental imagery. Cogn. Affect. Behav. Neurosci. 4, 251–259. https://doi.org/10.3758/CABN.4.2.251.